NOVA SCHOOL OF SCIENCE & TECHNOLOGY

DEPARTMENT OF CHEMISTRY

ANDREIA FILIPA MORAIS SIMÕES

BSc in Cell and Molecular Biology

RECOVERY AND PURIFICATION OF CUTIN FROM TOMATO BY-PRODUCTS FOR APPLICATION IN HYDROPHOBIC FILMS

MASTER IN BIOTECHNOLOGY

NOVA University Lisbon
March, 2022

NOVA SCHOOL OF SCIENCE & TECHNOLOGY

DEPARTMENT OF CHEMISTRY

RECOVERY AND PURIFICATION OF CUTIN FROM TOMATO BY-PRODUCTS FOR APPLICATION IN HYDROPHOBIC FILMS

ANDREIA FILIPA MORAIS SIMÕES
BSc in Cell and Molecular Biology

Adviser: Carla Maria Carvalho Gil Brazinha de Barros Ferreira, Researcher
NOVA School of Science and Technology, NOVA University of Lisbon

Co-adviser: Isabel Maria Rôla Coelhoso, Associate Professor with Habilitation
NOVA School of Science and Technology, NOVA University of Lisbon

MASTER IN BIOTECHNOLOGY

NOVA University Lisbon
March, 2022

RECOVERY AND PURIFICATION OF CUTIN FROM TOMATO BY-PRODUCTS FOR APPLICATION IN HYDROPHOBIC FILMS

To my mom and brother,

Acknowledgments

The writing of a thesis is without any doubt a journey, and one that is rarely done alone. In light of this, it seems only fair to embrace this opportunity and thank the people who shared this path with me.

First of all, I would like to thank my supervisor, Doctor Carla Brazinha, for giving me the opportunity to develop this very interesting work. For trusting me and giving me the means and freedom to conduct this study and test all the hypotheses that emerged along the way. I am grateful for all the help, the enthusiastic supervision and for vibrating with me at each result obtained.

I would also like to thank Professor Vítor Alves and Professor Isabel Coelhoso for their valuable contributions to this work. For sharing their vast knowledge with me in the form of thoughtful suggestions and for always showing availability and interest throughout this work.

I must also thank Cátia Gil, Bhavna Alke and Suchintan Mondal for taking time out of their busy schedules to share their knowledge with me and helping me develop some steps of this work.

A very special thanks has to go to the technician Mafalda Cadima. Thank you Mafalda for receiving me so warmly, for all the advice and for always ensuring that all conditions, safety and otherwise, were met for the development of the work. I am grateful to have met such a great and professional person.

I couldn't help but express my immense gratitude to Verónica Weng, Filipa Pires, Marisa Cardoso, and Bruno Pereira. They welcomed me with open arms and each of them marked my thesis journey in such a positive way. Besides their immense abilities and brilliant minds, they are also really kind people. I will forever remember Veronica's loyalty and willingness to help, Filipa's assertiveness and strength, Marisa's good heart and compassion, and Bruno's sense of humor and charisma.

I also want to thank Joana Salvada. I make her words mine in the sense that I thank her for all the times she listened to me and for all the words of encouragement she gave me. Writing a thesis was a wonderful adventure to share with you.

To my dear friends Catarina Toste, Ana Tomás, Jessica Pereira, Marta Neves, Alexandre Rocha and Mariana Fernandes for understanding and never charging my absence during the busiest months of the thesis. For always supporting me and offering me words of motivation. I am very grateful for your friendship.

Last but not least, and with a special place in my heart, I want to thank my wonderful mother and brother. I thank them for all their patience during these months, because they were the ones dealing with the most challenging side of a project as intense as this one. For their love and support and for always believing in me and my abilities.

Since it is impossible to mention all the people who in one way or another contributed to the development of this thesis, to all those who have not been mentioned, my most sincere thanks.

Abstract

Tomato pomace is a low-cost, renewable resource that recently has been studied for the extraction of a biopolyester of great interest – the cutin. This biopolyester is mainly composed of long-chain hydroxy fatty acids, which are considered excellent building blocks for the production of new hydrophobic biopolymers.

In this context, this thesis aimed the extraction and isolation of cutin in the form of monomers from tomato pomace, and its application in the production of hydrophobic cutin-based films.

A batch of tomato pomace composed of peels (63.62 ± 1.85% w/w), seeds (34.59 ± 2.51% w/w), fiber (1.80 ± 0.73% w/w) and with a moisture content value of 84.07 ± 0.42% (w/w) was used in this work as the raw material for the production of monomeric cutin extracts.

Several strategies for the isolation and depolymerization of cutin were explored. Strategies differed in the state of the raw material at the beginning of the extraction process, the existence of an initial tomato peel dewaxing step and type of solvent used for this purpose, type of alkaline hydrolysis and isolation method of cutin monomers. The extraction strategies tested in this study enabled the production of extracts enriched in fatty acids, such as 16-hydroxy-hexadecanoic acid, hexadecanedioic acid, stearic acid, linoleic acid, palmitic acid, octadecanedioic acid and oleic acid.

Cutin and chitosan-based films were successfully produced from the cutin extracts and from commercial chitosan by the casting method.

Two types of films were produced — blend of cutin and chitosan and bilayer films. Cutin and chitosan blend films were the most malleable and homogeneous.

Cutin and chitosan blend films were characterized regarding its thickness (0.103 ± 0.004mm and 0.106 ± 0.005mm), color, water contact angle (93.37 ± 0.31° and 95.15 ± 0.53°) and water vapor permeability ((3.84 ± 0.39) $x10^{-11}$ mol.m/m^2sPa and (6.20 ± 2.44) $x10^{-11}$ mol.m/m^2sPa).

Keywords: Tomato pomace, Cutin, Fatty acids, Chitosan-cutin blend films, Chitosan-cutin bilayer films, Food packaging, Sustainability.

Resumo

O repiso de tomate é um recurso renovável e de baixo custo, que recentemente tem sido estudado para a extracção de um biopoliéster de grande interesse — a cutina. Este biopoliéster é composto maioritariamente por ácidos gordos de cadeia longa com grupos hidroxilo, e são considerados excelentes monómeros para a produção de novos biopolímeros hidrofóbicos.

Neste âmbito, esta tese teve como objetivo a extracção e isolamento de cutina sob a forma de monómeros, a partir de repiso de tomate, e a sua aplicação na produção de filmes hidrofóbicos.

Um lote de repiso de tomate constituído por peles (63,62 ± 1,85%), sementes (34,59 ± 2,51%), fibras (1,80 ± 0,73%) e com um teor de humidade de 84,07 ± 0,42%, foi utilizado para a produção de extractos monoméricos de cutina.

Foram exploradas várias estratégias para o isolamento e despolimerização de cutina. As estratégias diferiram no estado da matéria-prima no início do processo de extracção, na existência de uma etapa inicial de remoção de ceras das peles de tomate e do tipo de solvente utilizado para este fim, do tipo de hidrólise alcalina e do método de isolamento de monómeros de cutina. As estratégias de extracção testadas neste estudo permitiram a produção de extractos enriquecidos em ácidos gordos, tais como ácido 16-hidroxi-hexadecanóico, ácido hexadecanodióico, ácido esteárico, ácido linoleico, ácido palmítico, ácido octadecanodióico e ácido oleico.

Películas de cutina e quitosano foram produzidas com sucesso, a partir dos extractos de cutina e de quitosano comercial, pelo método de *casting*.

Foram produzidos dois tipos de películas — películas compósitas de cutina e quitosano e películas de dupla-camada. As primeiras foram as mais maleáveis e homogéneas.

As películas compósitas de cutina e quitosano foram caracterizadas em relação à sua espessura (0,103 ± 0,004mm e 0,106 ± 0,005mm), cor, ângulo de contacto com a água (93,37 ± 0,31° e 95,15 ± 0,53°) e permeabilidade ao vapor de água ((3,84 ± 0,39) $x10^{-11}$ (mol.m/m^2sPa e (6,20 ± 2,44) $x10^{-11}$ (mol.m/m^2sPa).

Palavras-chave: Repiso de tomate, Cutina, Ácidos gordos, Películas compósitas de quitosano e cutina, Películas dupla-camada de quitosano e cutina, Embalagens alimentares, Sustentabilidade.

Table of Contents

List of Figures

List of Tables

List of Abbreviations

a_w – Water Activity

FAO – Food and Agriculture Organization

GC-FID – Gas Chromatography with Flame Ionization Detection

MC_{wb} – Moisture Content (wet basis)

MWCO – Molecular Weight Cut-Off

PE – Polyethylene

PES – Polyethersulfone

PET – Polyethylene Terephthalate

PFA – Perfluoroalkoxy Alkane

PLA – Polylactic acid

PP – Polypropylene

PS – Polystyrene

PVC – Polyvinyl Chloride

RH – Relative Humidity

UV-Vis – Ultraviolet-Visible

WCA – Water Contact Angle

WVP – Water Vapor Permeability

1. Introduction

Currently, according to the Food and Agriculture Organization (FAO) of the United Nations, about one-third of all food resources produced for human consumption is lost [1]. This large fraction is due to the fact that food production is a wasteful process, with significant losses along its value chain, from crop residues, through processing, to sale and consumption [2]. Food processing is one of the points on the food chain that largely contributes to this problem, through the annual production of an enormous amount of waste and by-products [3]. In addition to representing a substantial waste of other resources, such as land, water, energy and labor, by-products of food processing are also a source of economic loss for the industries due to the cost of their disposal (e.g. costs associated with drying, storage and shipment) [1].

One of the possible solutions to be considered is to use such wastes as low-cost substrates to produce value-added products [1], [3]–[5].

An example of this valorization can be observed in the milk industry. Whey is the main by-product obtained by the dairy industry, with an annual whey production of 40 million tonnes in the European Union. [6] About 50% of residual whey is being valorized as a source of high-added-value compounds for the food or pharmaceutical industries, such as proteins of high biological value, lactose, lactic acid, minerals, etc. [7].

The fruit and vegetable processing industries also generate a huge amount of waste every year [5]. These residues are extremely diverse due to the use of a wide variety of fruits and vegetables, representing excellent resources for a diversity of compounds, such as proteins, peptides, polysaccharides, dietary fiber, polyphenols, antioxidants, natural pigments, etc. [3], [5].

Among many others, the tomato processing industry is a good example of this. Several applications have been exploited for the residue that arises from the tomato processing activity, designated as tomato pomace. [3], [5], [8] Among them are the use of this by-product as a supplement for animal feed [9]–[11], due to its high protein content, and for the extraction of lycopene, an antioxidant, for incorporation into food, pharmaceuticals and cosmetics [12]–[14]. More recently, the possibility of using this by-product for the extraction of a biopolymer, cutin, for the production of renewable materials has been explored [8], [15], [16].

1.1 Tomato

Tomato (*Solanum lycopersicum*) is one of the most produced and extensively consumed crops, after potatoes, with a worldwide rising production of 180 million tonnes in 2018, 183 million tonnes in 2019 and 186 million tonnes in 2020 [17], [18].

The increased demand and consumption of both fresh tomatoes and tomato-based products (paste, juice, sauces, canned peeled tomatoes, etc.) has been attributed not only to the enjoyable taste and the multiple forms this fruit can be eaten but also to the already many reported health benefits associated with it. Several studies have shown a link between the consumption of this fruit and a reduction in the risk of inflammatory processes, carcinogenesis (e.g. prostate cancer) and different chronic diseases (e.g. cardiovascular diseases), constipation prevention, detoxification of body toxins, maintaining bone structure, etc. [14], [19], [20]

Some important traits that other model plants, such as *Arabidopsis* and rice, do not have, make the tomato plant and the fruit itself a great object of study. Features such as a fleshy fruit, a sympodial shoot and compound leaves can be studied through this plant. [21]

Based on the fruit's final use, tomato cultivation can be divided into two categories: cultivation for fresh consumption and processing tomato cultivation [18], [22]. Depending on the purpose of cultivation different tomato varieties are chosen and different growing conditions are used [22].

For fresh consumption, tomatoes are grown both in greenhouses and open fields and the selection of the varieties to be cultivated must meet several requirements, including outdoor growing (if applicable), high yield, early maturity, external fruit quality (from shape to color, to homogeneity), internal fruit quality (e.g. flavor, sweetness, and juiciness), extended shelf life, adaptability to different cropping systems, and resistance to biotic and abiotic stresses. Other characteristics are required if the cultivation of these varieties is carried out in a greenhouse, such as being adaptable to long harvesting periods, low temperature and light intensity, etc. Some examples of the tomato varieties for fresh consumption are classic round, beefsteak, cocktail and cherry (**Figure 1.1**). [21], [22]

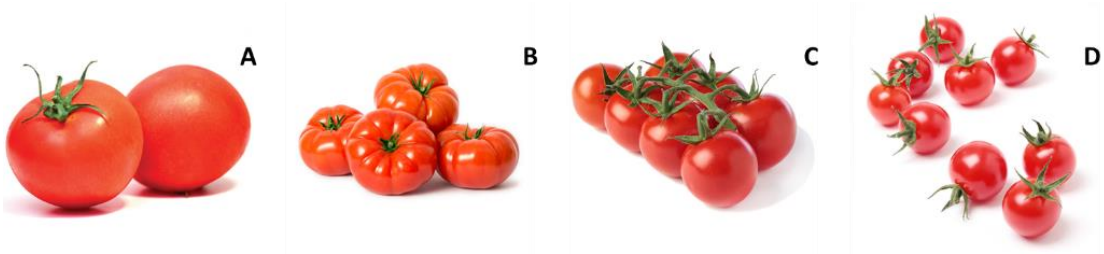

Figure 1.1 - Fresh consumption tomato varieties. A – Classic round; B – Beefsteak; C – Cocktail; D – Cherry. [23]

In production for processing, tomatoes are grown only outdoors (open field), lately preferably by direct seeding instead of using transplants, and the varieties are chosen based on other criteria, including compact plant growth, grouped flowering and ripening, easy detachment of the fruit from the plant, fruit shape and size homogeneity, easy peeling, thick and firm pericarp, among others. Some examples of the varieties cultivated for processing are plum and baby plum tomatoes (**Figure 1.2**). [21], [22]

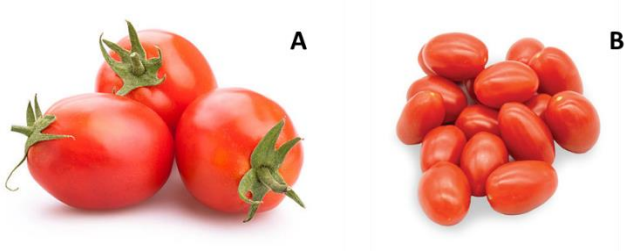

Figure 1.2 - Processing tomato varieties. A – Plum; B – Baby plum. [23]

Botanically, tomatoes are described as berries that contain seeds within a fleshy pericarp. The tomato fruit is composed from the outside to the inside as follows: skin/peel (epicarp), which

encapsulates the red layer (exocarp), followed by the mesocarp and endocarp, as represented in **Figure 1.3**. [21]

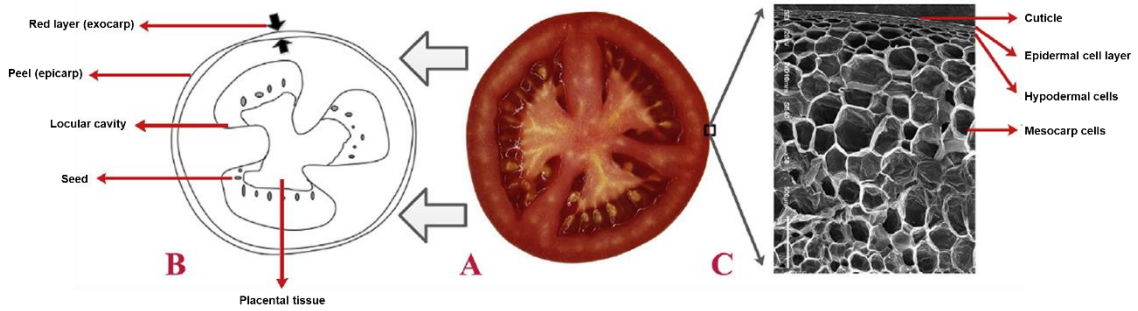

Figure 1.3 - Structure of tomato fruit. A – Cross-section image. B – Diagrammatic drawing. C – Fine structure of the tomato outer layer. Adapted from [11].

Exocarp, mesocarp and endocarp make up the pericarp. The seeds are attached to tissue that is referred to as placental tissue and are surrounded by jelly-like parenchyma. These are found in the locular cavities. The term “pulp” when used refers to the placental and locular tissues. A fresh fruit's pulp typically makes up less than a third of its mass. The terms "skin" and “peel” are not botanical terms; however, these are widely used throughout the existing literature on this subject for simplification and refer to the outer layer of the tomato. In more detail, the tomato peel is composed of a thin but very important barrier designated cuticle, a single layer of epidermal cells, and two to four layers of hypodermal cells with unevenly thickened walls. In contrast to the epicarp, the red layer is constituted of much larger parenchymatous cells. [11], [20], [21], [24]

Tomato is an extremely water-rich fruit. Generally, the dry matter content of tomatoes ranges from 4 to 7.5%. Variations in tomato dry matter content can be attributed to several factors, including ripeness, seasonality, and tomato genotype. The value of dry matter decreases with fruit development, is higher in summer than in winter and is lower for beefsteak than for cherry tomato. [21]

The organoleptic properties of the final fruit, such as flavor and texture, but also its nutritional value depend on the percentage of dry matter of these fruits, its composition (sugars, acids, cellulose, proteins, antioxidant compounds, and minerals), as well as on the ratio between sugars and acids and their dilution by water. [21]

Tomato fruit is mainly composed of soluble sugars, organic acids, amino acids, vitamins, carotenoids and polyphenols (**Figure 1.4**).

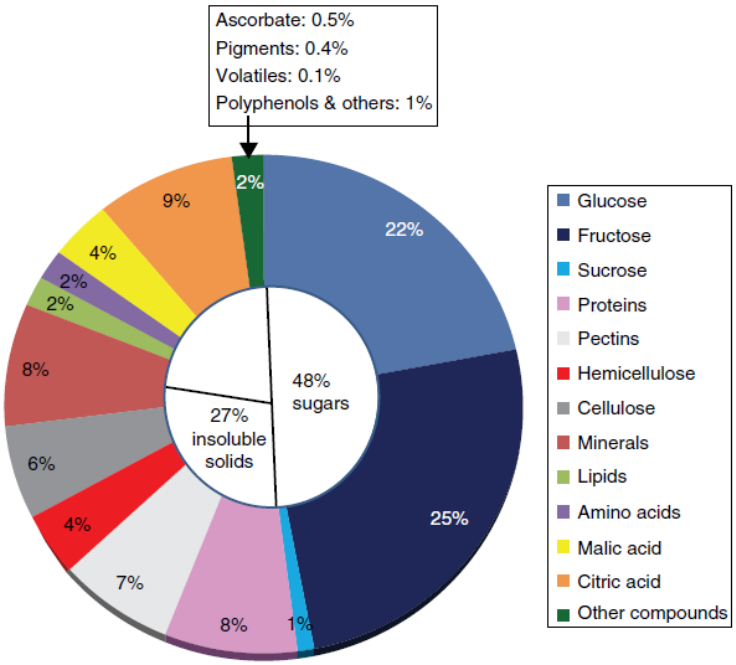

Figure 1.4 - Schematic representation of tomato dry matter composition. [21]

Sugars most frequently found in tomatoes are fructose, glucose, and to lesser extent sucrose. Malic acid and citric acid are the most representative organic acids, and glutamic acid and leucine are the most expressive amino acids. About 50% (w/w) of tomato dry matter content is sugars and about 15% is organic acids and amino acids. Vitamin C (ascorbic acid) is the most abundant, however, vitamin B-complex, A, E and K are also present. Regarding carotenoids, lycopene and β-carotene are by far the most abundant and are the principal responsible for tomatoes' red color, but others are also present, such as, phytoene and phytofluene. The main polyphenols in tomatoes are chlorogenic acids and flavonoids. [14], [21], [24]

1.1.1 Cultivation and Transformation of Tomato

The WPCT (World Processing Tomato Council) estimated that in 2020 the countries that belong to AMITOM (Association Méditeranéenne International de la Tomate), of which Portugal is a member, produced a total of 17.262 million metric tonnes of tomatoes for processing, and that global production reached 38.402 million metric tonnes. In 2021, through a preliminary analysis, it is estimated that the global production may have reached 38.733 million metric tonnes and that 1.596 million metric tonnes of these correspond to Portugal's production. [25]

Tomato processing is the set of processes that allows the transformation of tomatoes into several by-products, such as whole or diced canned peeled tomatoes, tomato juice, paste, purée, ketchup, sauce, salsa, etc. [24]

After being harvested, mechanically in the case of processing tomatoes, and manually for fresh consumption tomatoes, the former are then transported to the plant units. Once there, the tomatoes are unloaded and routed, e.g. hydraulically, to a washing and sorting point. The washing step removes any soil that may have clung to the tomatoes and the sorting step is aimed to

eliminate defective and undesirable fruits. Sorting can be manual or automated. An example of an automated method consists of an X-ray and optical sorter. [26], [27] The next step consists in removing the peel from the tomatoes with steam or lye peeling (a chemical peel using an alkaline heated solution that dissolves the peels, such as sodium hydroxide or potassium hydroxide) followed by mechanical removal of the peels [28]. At this stage, a new control step is made to exclude defective fruit or fruit whose peels have not been removed. From this stage on, the tomato processing steps will be different depending on the type of tomato-based product the company wants to produce. [26], [27]

If the goal is to produce whole peeled tomatoes, the intact peeled tomatoes are used. But if the goal is to produce diced tomato, then the peeled tomatoes are diced and tomato juice is added, followed by steam sterilization. Finally, to ensure that the sterile product is not contaminated, it is aseptically packed. [24]

The production of tomato juice or paste is somewhat different. Washed and sorted tomatoes are chopped into tiny pieces. Then, an enzyme inactivation is induced by a cold break (65–70°C) or hot break (>90°C) in a chopper box and tubular heater. The removal of peels and seeds is done by passing the material through a set of sieves. To avoid wasting tomato, the removed materials are compressed to recover some lost juice. The juice is then centrifuged to remove any peels and seeds that might come with it. To turn the juice into a paste, concentration using an evaporator is performed. The final product is finally packaged aseptically. [24]

1.2 Tomato Industry Waste

1.2.1 Characterization

As mentioned, tomato processing generates waste products. This waste has been nominated as tomato pomace. Throughout the literature, it is reported that tomato pomace on average accounts for 3–5% (wet basis) of fresh tomato. [11], [24]

This by-product is characterized, in general, by having a high-water content. Del Valle *et al.* [29] reported moisture contents ranging from 64.31 to 92.55% (w/w) for wet tomato pomace collected from different production stages in a factory. Lavelli and Torresani [12], by simulating in laboratory conventional (use of heat-stabilized fruit) and innovative (use of raw fruit) tomato processing technologies, obtained water content values of 90.0 ± 0.2% (w/w) and 92.7 ± 0.1% (w/w), respectively. By comparing tomato by-products to unprocessed tomatoes, Kalogeropoulos *et al.* [30] determined moisture contents of 73.85% (w/w) and 94.69% (w/w), respectively. A slightly higher value was reported by Bhat and Ahsan [31] who stated that the fresh tomato pomace batch studied by them contained 87.63 ± 0.12% (w/w) of moisture. In 2019, Silva *et al.* [32] through the characterization of 6 batches of tomato pomace, all originated from different producers, obtained a range of moisture content values from 62.27 to 70.14% (w/w) (**Table 1.1**).

Table 1.1 - Water/moisture content values, % (w/w), of different batches of tomato pomace reported in the literature.

	Del Valle *et al.* [29]	**Lavelli and Torresani** [12]	**Kalogeropoulos *et al.*** [30]	**Bhat and Ahsan** [31]	**Silva *et al.*** [32]
Moisture content % (w/w)	64.31–92.55	90.0 ± 0.2 92.7 ± 0.1	73.85 ± 0.24	87.63 ± 0.12	62.27 ± 0.54– 70.14 ± 0.37

From the data gathered in **Table 1.1**, it can be concluded that the moisture content in the tomato processing by-products varies with several factors, including processing stage, type of processing technology, or even differences in the raw material. This is supported by Silva *et al.* [32], who provides a direct example of how differences in processing conditions can lead to higher moisture content. Namely, the use of a hydraulic method by some factories to transport the tomato waste for final disposal. It is only logical that the tomato pomace produced by a factory whose method of transporting this pomace is done using water will have a higher moisture content than a tomato pomace produced by a factory that does not use water. [29], [32] The water content is used by some factories to measure the efficiency of tomato flesh and pulp extraction, as a critical control point. If the moisture content of the pomace is above a threshold specified by the factory, this means that the flesh and pulp are not being completely extracted, and in that case, it is necessary to optimize the extraction process [32].

The proportion of peels and seeds in tomato pomace varies slightly among the lots analyzed and reported in the literature (**Table 1.2**), but in all studies, and consequently, in all lots, the percentage of peels was higher than the percentage of seeds.

Table 1.2 - Composition in peels and seeds, % (w/w), of different batches of tomato pomace reported in the literature.

Fraction, % (w/w)	**Kaur *et al.*** [33]	**Nour *et al.*** [34]	**Silva *et al.*** [32]	**Costa *et al.*** [13]
Peels	56	77.8	57.5 ± 1.7–65.3 ± 1.9	71
Seeds	44	22.2	34.7 ± 1.9–42.5 ± 1.7	29

1.2.2 Applications

The fact that each of the tomato pomace fractions has a different chemical composition opens a range of possible uses for this raw material. Currently, the valorization of this residue is done essentially through incorporation as a supplement in animal feed, human food, and recovery of added-value compounds (**Figure 1.5**). [11]

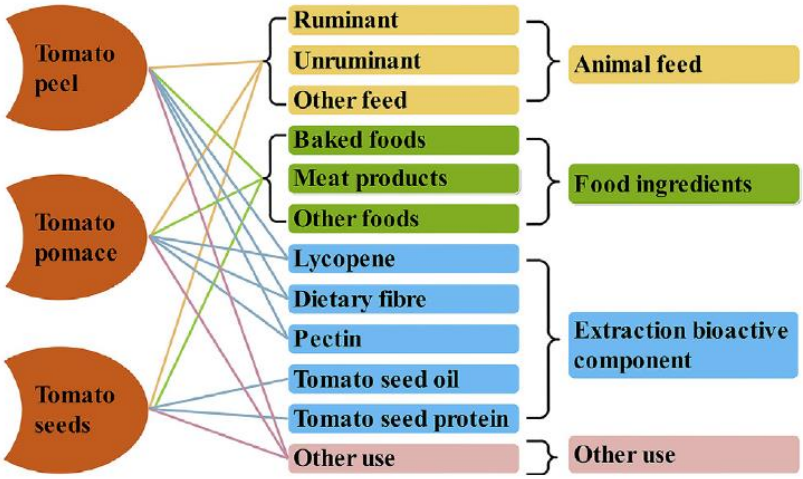

Figure 1.5 - Schematic representation of the current uses of tomato pomace and its fractions.[11]

The incorporation of tomato pomace as a supplement to animal feed, or as a complement to animal pasturing, is due to its nutritional component, especially the high protein content present in the seeds. To evaluate the effects of this incorporation, several case studies with a variety of animals have been developed, including cows, pigs, hamsters, chickens, carp, etc. From these case studies, somewhat inconsistent and contradictory results have been reported. [11] While Yuangklang *et al.* [10] reported a 15% retardation in the growth of cattle in the course of adding 11.2% of dried tomato pomace to the usual ration given to these animals, Gebeyew *et al.* [35] observed a favoring of sheep growth and an improvement of the resulting carcass quality when the usual hay-based feed of these animals was supplemented with dried tomato waste. The data resulting from these case studies allowed to perceive that the effectiveness of the tomato pomace incorporation depends largely on the case and that it varies with several factors, including the animal species, the quantity of tomato pomace added to the feed, the relative nutritional value of the normal feed compared to the tomato pomace, the condition of the incorporated tomato pomace (fresh, dry or ensiled) and the length of the feeding period. [11]

The high content of lycopene, phenols, dietary fiber, unsaturated fatty acids, and essential amino acids of the tomato pomace has led to its incorporation in the form of powder as a supplement in many human food products, including in cookies, bread, pasta, hamburgers, sausages, tomato paste, etc. On one hand, the incorporation of this raw material improves the nutrient content of the food product, as well as provides antioxidant properties to the formulated food products, but on the other hand, it can also change fundamental food characteristics such as texture and sensory traits. [11]

Alternatively to the incorporation of tomato pomace as a whole (or of its fractions), there is also the possibility to extract from it only the compounds of greatest interest, such as lycopene, dietary fiber, pectin, proteins, oil, etc. In this case, the use of adequate technologies to minimize deterioration of those compounds should be implemented (e.g. the sensitive lycopene has to be extracted under mild temperature conditions) [36]. Once extracted and purified, these compounds

can be applied in the food industry, but also in other industries such as pharmaceutical/cosmetic and textile. [11]

In a very recent study, Costa *et al.* [13] investigated how changes in the odor and color of cosmetic products induced by incorporation of lycopene-enriched extracts, obtained from tomato pomace, can be perceived by the public. The authors concluded that the willingness or reluctance to buy a personal care product does not depend only on its organoleptic properties. They observed that providing information about the composition of the product, such as the presence of an antioxidant compound, can lead to a greater likelihood of it being purchased.

Another possible application is the dyeing of fabrics with the pigments extracted from tomato by-products in the textile industry. [37]

Other possible uses reported for this tomato pomace are the production of biofuels such as biodiesel and biogas [38], [39], as well as can serve as a carbon source for the production of certain bioproducts by specific strains, such as laccase, xylanase, vitamin B_{12} and bioflavour [40]–[43].

Although not represented in **Figure 1.5**, several sources also mention the direct use of tomato pomace as a soil fertilizer [18], [44], [45], but some also warn of the environmental risk that this act can pose. The high-water content of this pomace is conducive to its rapid spoilage. [24]

1.3 Tomato Cutin

1.3.1 Tomato's Cutin Location

As mentioned earlier, the tomato peel is composed of a very important protective layer known as the cuticle. The cuticle is an essential structural element not only for the fruits of a plant, such as tomatoes but also for the flowers, leaves and stems. This structural element not only acts as a primary barrier protecting the plant and fruit tissues against biotic stresses (microorganisms, pests, etc.), abiotic stresses (radiation, temperature, relative humidity, etc.) and mechanical stresses but also regulates gas exchange and prevents water loss from internal tissues. [16], [46]–[49]

This cuticle is composed mostly of cutin, an insoluble polyester discussed in more detail later on, and also polysaccharides. These are derived from the epidermal cell wall and are mainly cellulose, hemicelluloses, and pectin. Waxes are also constituents of this and exist in two forms: epicuticular waxes, accumulating on the outer surface of the epicarp, and intracuticular waxes, embedded in the cutin matrix (**Figure 1.6**). [16], [48]–[50] The wax fraction corresponds to mixtures of C20–C40 n-alcohols, n-aldehydes, n-alkanes, fatty acids and esters. Also, in this wax fraction the presence of cyclic compounds such as triterpenoids is reported. Finally, in smaller quantities within the cutin matrix are phenolic compounds, mainly hydroxycinnamic acid derivatives and flavonoids. [46], [50]

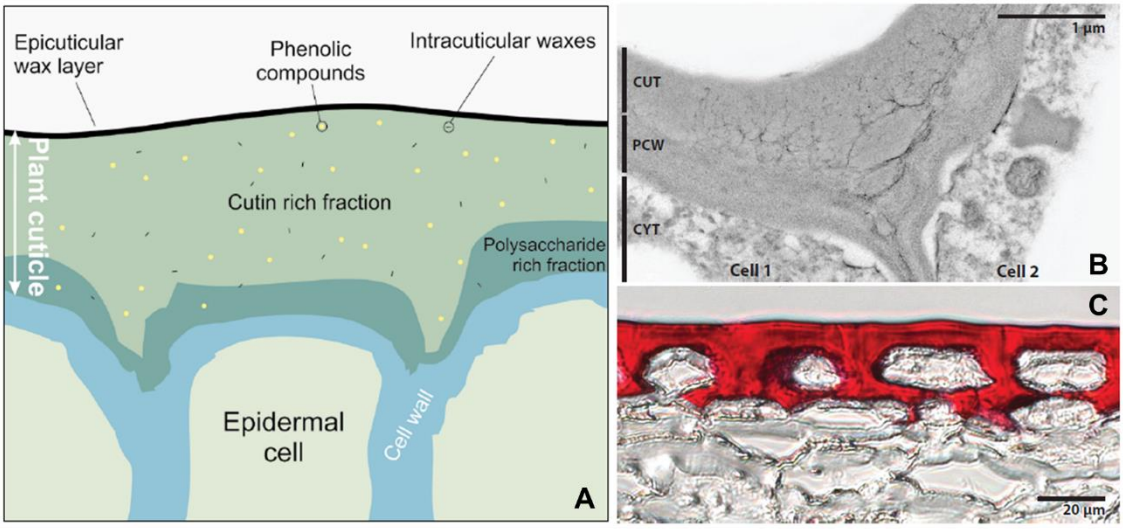

Figure 1.6 - Plant cuticle. A – Schematic diagram of the cross-section of a plant cuticle [50]; B - A transmission electron microscopy (TEM) image of tomato fruit tissue [51]; C - Image of mature tomato fruit tissue, with the cuticle stained red. [51] Legend: CUT – cuticle; PCW – polysaccharide cell wall; CYT – cytoplasm.

1.3.2 Structure and Physical-Chemical Characteristics

Cutin represents 40 to 85% of the cuticle's dry weight. [48] This polymer is made up of long-chain (mainly C16 and C18) hydroxy fatty acids linked together by ester bonds. Many of these monomers are polyhydroxylated, containing a terminal hydroxyl group, but also medium-chain hydroxyl groups. The presence of monomers with epoxy and oxo mid-chain groups is also reported. The C16 dihydroxy fatty acids typically have the second hydroxyl group at C-10, C-9, C-8 and/or C-7 and the C18 dihydroxy fatty acids at C-9 and C-10. Cross-linking via these hydroxyl groups allows the formation of a rigid three-dimensional matrix characteristic of cutin. The presence of aromatic groups, dicarboxylic acids, and glycerol are also reported, although in smaller amounts. [15], [48], [52]–[54]

Benítez *et al.* [8] reported the monomer composition of cutin extracts produced from dewaxed tomato peels through alkaline hydrolysis followed by a precipitation process. The most predominant monomer was 10,16-dihydroxyhexadecanoic acid (43.3%), followed by linoleic acid (16.1%) and oleic acid (11.9%). Hydroxy diacids (e.g. 7/8-hydroxyhexadecanedioic acid), mono hydroxy acids (e.g. 16-hydroxyhexadecanoic acid) and saturated acids (e.g. palmitic and *p*-coumaric acids) were also present in the investigated extracts (**Figure 1.7**). [8]

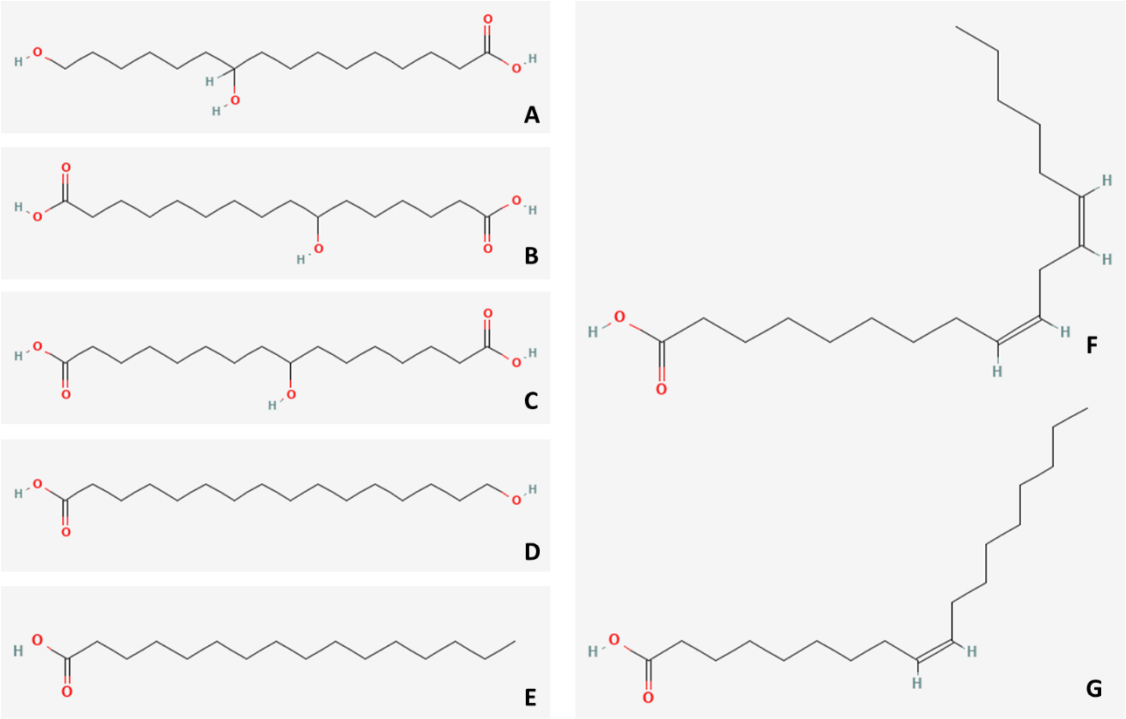

Figure 1.7 - Chemical Structure of cutin monomers. A - 10,16-dihydroxyhexadecanoic acid [55]. B - 7-Hydroxyhexadecanedioic acid [56]. C – 8-Hydroxyhexadecanedioic acid [57]. D - 16-Hydroxyhexadecanoic acid [58]. E – Palmitic acid [59]. F – Linoleic acid [60]. G – Oleic acid[61].

In 2019, Cifarelli *et al.* [48] produced depolymerized cutin extracts from tomato peels using four different methods. Briefly, these consisted of alkaline hydrolysis, alkaline hydrolysis with purification (recovery of water-soluble material), in a sodium carboxylate route and an alkaline peroxide route. In all extracts, regardless of the extraction method used, the major monomer was 10,16-dihydroxyhexadecanoic acid (62.4 ± 15.1 – 82.2 ± 3.7%). Although in smaller amounts, other isomers such as 9,16-dihydroxyhexadecanoic acid, 8,16-dihydroxyhexadecanoic acid and 7,16-dihydroxyhexadecanoic acid were also present. The second most representative monomer was 16-hydroxyhexadecanoic acid (2.2 ± 0.5 – 5.6 ± 0.9%). C18-fatty acids (e.g. octadecanoic acid), epoxy-hydroxy monomers (e.g. 9,10-epoxy-18-hydroxyoctadecanoic acid), saturated acids and some unsaturated acids (e.g. oleic acid) were also identified. [48]

Moreira *et al.* [53] reported the fatty acid composition of three different tomato-related matrices: untreated tomato peels, cutin samples extracted from tomato peels with an enzymatic method, and cutin samples extracted with cholinium hexanoate or 1-butyl-3-methylimidazolium acetate. In general, the monomeric compositions of all the extracts were similar. The most abundant compound in all matrices was the polyhydroxy acid 10,16-dihydroxyhexadecanoic acid (58.12 ± 1.89 – 63.24 ± 0.98%), followed by the dicarboxylic acid 8/9-hydroxyhexadecanedioic acid (9.53 ± 0.23 – 17.66 ± 0.20%) and the 16-hydroxyhexadecanoic acid (5.38 ± 0.16 – 15.71 ± 0.68%). Compounds such as hexadecanoic acid, 16-hydroxy-10-oxohexadecanoic acid and 9,10-epoxy-18-hydroxyoctadecenoic acid were also present, but to a lesser extent. [53]

Due to its composition, cutin is described as a hydrophobic, high elongation at breaking point, infusible, non-toxic, UV-blocking biopolymer. [8] In addition, cutin is also biodegradable. De Vries *et al.* [62] showed that enzymes, such as cutinases (secreted by soil microorganisms and fungi), can degrade cutin after three to eight months, depending on time and site conditions (i.e. season, soil characteristics, and microbiota). [62]

1.3.3 Cutin Depolymerization Methods

Production of cutin bioplastics requires the isolation of the cuticle from the raw materials (such as plant leaves, fruit peels, etc.). Cutin extraction is commonly achieved by its depolymerization, i.e., the breakdown into its constituent monomers, rather than extracting it as a whole. From the literature reported on this subject, it is noticeable that the cutin depolymerization procedure has been evolving from more complex, expensive, time-consuming and non-green methods to simpler, more affordable, faster and more sustainable methods. [15]

Initially, cutin isolation was accomplished by degrading the polysaccharide-rich fraction near the cell wall of the material by immersing it in an enzymatic solution of pectinases, cellulases, and hemicellulases. Chemical extraction (e.g., ammonium oxalate/oxalic acid or zinc chloride/hydrochloric acid) was also used as an alternative to enzymatic degradation. Isolated cuticles were dewaxed with organic solvents (e.g. chloroform, methanol, hexane, or different mixtures of the previous) and remaining polysaccharides still not extracted were removed by acid hydrolysis. Depolymerization itself, i.e. cleavage of the ester bonds in the cutin matrix to obtain monomers, was performed in several ways, including alkaline hydrolysis, with sodium hydroxide or potassium hydroxide solutions and transesterification, with methanol containing boron trifluoride or sodium methoxide. [15]

Currently, simpler methodologies include direct hydrolysis of the material. Montanari *et al.* [63], produced monomeric cutin extracts by direct hydrolysis of tomato peels with an alkaline sodium hydroxide solution. Marc *et al.* [64] also produced extracts enriched in cutin monomers from tomato peels by alkaline hydrolysis, however, prior to cutin depolymerization peels were dewaxed with a mixture of acetone and ethanol.

1.3.4 Cutin-Based Hydrophobic Films

Cutin's hydrodynamic, thermal and mechanical properties have prompted consideration of the applicability of this material for the production of bioplastics, as an alternative to the use of conventional plastics. [8]

Manrich *et al.* [65] produced cutin and pectin films with monomeric cutin/pectin ratios of 50/50 and 25/75. In this study, pectin was chosen as the binding agent due to its excellent film-forming properties. The films produced demonstrated to mimic tomato peel in terms of mechanical strength and thermal stability but were slightly affected by moisture, which would imply a short period of utilization if used as water-resistant wraps. Meanwhile, Wang *et al.* [66], also produced monomeric cutin and pectin films but modified them further by spraying them with an emulsion of

beeswax in ethanol. As a result, repellency for various food liquids was achieved (e.g. contact angle of 146° with coffee and 153° with water).

In 2018, polymer films from a monomeric cutin mixture were prepared by Benítez *et al.* [8] through a melt-polycondensation method without catalyst at 150ºC. These were characterized as hydrophobic (water contact angle values near 90°), thermally stable (decomposition onset temperature above 300°C), infusible (no melting points detected) and amorphous. [8]

However, cutin-based films haven't been exclusively produced from tomato extracted cutin. Ye *et al.* [67] incorporated lotus leaf extracted and cutin in a low-methoxyl pectin and chitosan film to produce hydrophobic composite films. The incorporation of this lotus leaf monomeric cutin into the films led to an increase in hydrophobicity, which was perceived through an increase in the water contact angle value (61.8º for films without cutin and 90.3º for films produced from a film-forming solution containing 1.5% (w/w) of cutin), as well as an increase in mechanical properties and thermal stability. The water vapor permeability of films increased with the cutin amount, which the authors justified as a possible exceeding of the optimal content of cutin in the films. [67]

Cutin and polysaccharide films have not been the only type of films reported so far. Last year, Hood *et al.* [68] reported the production of films made from zein, an important corn storage protein, and cutin, once again extracted from tomato peels. The added cutin improved the water repellency and mechanical properties. This was verified by an increase in the water contact angle from films containing only 30% (w_{cutin}/w_{zein}) to films containing 60% cutin (w_{cutin}/w_{zein}) and by obtaining homogeneous and robust films with better performance under bending mechanical stress. [68]

1.4 Food Packaging

1.4.1 Conventional Plastics (Petroleum-Based Polymers)

The growth of the population has inevitably led to an increase in food demand. Since food packaging is essential for its preservation, it is understandable how the increased demand for food has led also to an increase in the volume of packaging waste. [69]

The purpose of food packaging is, as mentioned, to preserve food, which among other factors includes retard product spoilage, retaining the beneficial effects of processing, extending shelf life, and maintaining the quality and safety of food. [69]–[71] This implies that the packaging must provide protection on a chemical, biological and physical level. At a chemical level, the packaging must minimize changes in the product that arise from exposure to gases such as oxygen, moisture and light. Therefore, to prevent food spoilage, the oxygen permeability (OP) and water vapor permeability (WVP) values of the packaging material should be as low as possible. Biologically, it must provide a barrier between food and microorganisms (pathogens and spoilage agents), insects, rodents, etc. [70], [71] As for physical protection, it must be able to protect food from mechanical damage (e.g. shock, vibration, etc.) that can occur, for example, during transport. [71]

Of the different material types, paper, cardboard and plastic were the most common types of packaging waste in 2019 (**Figure 1.8**). [69], [70], [72]

Figure 1.8 - Schematic representation of the percentage of packaging waste generated by type of packaging material. [72]

As is well known, of these two the one that represents a greater environmental hazard is plastic. Six types of plastics, or rather six types of petroleum-based polymers used to produce plastic, stand out in the market: polyethylene (PE), polypropylene (PP), polyvinyl chloride (PVC), polyurethane (PUR), polyethylene terephthalate (PET), and solid polystyrene (PS). [54], [70], [73]

Plastics improve the quality of human life due to their numerous properties such as lightweight, corrosion resistance, low cost, easy processing, and a range of applications so wide that range from food packaging to building and construction. [54], [71] Despite the many characteristics that make plastics extremely useful materials, their continued use has major disadvantages. The easiest to point out is clearly the enormous production of waste, as only a very small part is recyclable, the rest being incinerated or ending up on land or in the sea. [54], [69]

1.4.2 Bioplastics (Biobased & Biodegradable)

A bioplastic, according to the Bioplastics Organization, is a plastic material that is either biobased (partially or fully), biodegradable, or both (**Figure 1.9**). The term “biobased" refers to the fact that the material is derived from biomass (e.g. corn, cellulose, etc.) and the term "biodegradable" means that the material can be biologically degraded to natural elements (water, carbon dioxide, methane, etc.). [69], [70], [74]

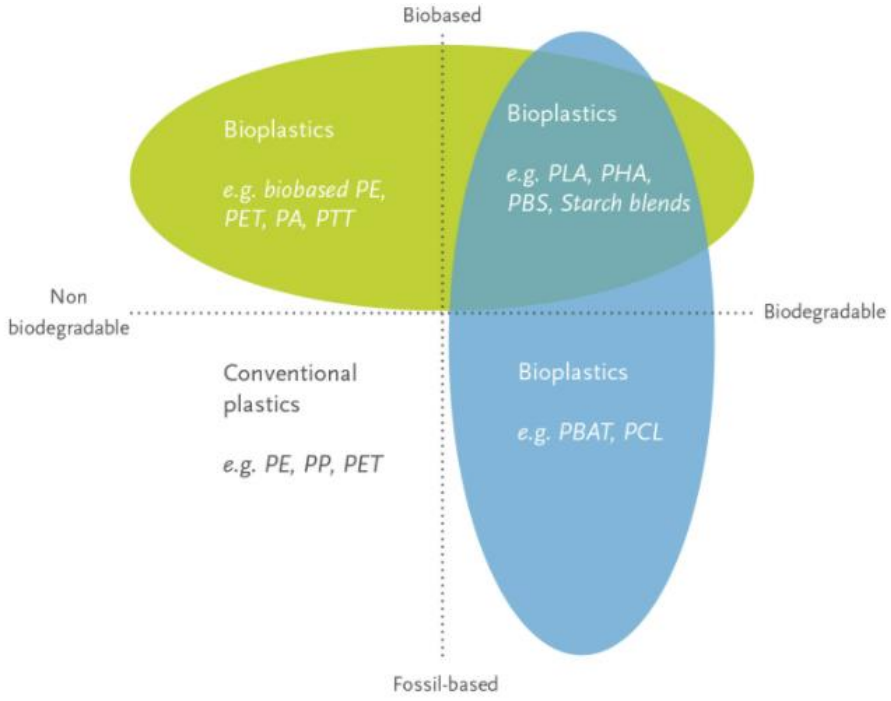

Figure 1.9 - Schematic diagram of the bioplastics family grouped by category. [74]

Compared to conventional plastics (petroleum-based plastics), bioplastics have two major advantages: save fossil resources by using biomass that regenerates (renewable resources) and which value may not be fully exploited and provide the unique potential of carbon neutrality. Biodegradability is an extra property of certain types of bioplastics.

Biobased non-biodegradable polymers include biobased PET (or bio-PET) partially produced from plant-derived ethylene glycol (e.g. sugar cane) [75], biobased PTT (polytrimethylene terephthalate) partially produced from 1,3-propanediol obtained by fermentation [76], and biobased PA (polyamide), such as PA11, produced from castor oil-derived 11-aminoundecanoic acid [76].

Biobased biodegradable polymers can be derived from different sources: from biomass (e.g. chitosan, cellulose, lignin, starch and cutin), from microorganisms (e.g. PHA - polyhydroxyalkanoates) and biotechnology (e.g. PLA - polylactic acids). [54], [70]

1.4.3 Chitosan-Based Films for Food Packaging

Chitosan has been extensively studied in recent decades. Recently, the major focus is the production of films and coatings for the preservation of fresh and processed foods, due to its excellent properties of antimicrobial activity, nontoxicity, biocompatibility, biodegradability, etc. [77]–[79]

It is a derivative of chitin after deacetylation that can be extracted from shrimp shells and other crustaceans. Structurally, it is a linear polysaccharide composed of randomly distributed β-(1→4)-linked d-glucosamine and N-acetyl-d-glucosamine. [77]–[80]

Pure chitosan films have already been tested in the preservation of various foods, including bananas, carrots, tomatoes, fish, blueberries, among others. Delay of qualitative and

nutraceutical alterations, prevention of the growth of microorganisms, antioxidant activity maintenance, and extended shelf life were some of the positive effects observed on food when using chitosan-based films. [77], [78]

This macromolecule not only enables the production of pure films, but it is also a suitable compound to combine with other biopolymers to produce chitosan/biopolymer films. Some of these biopolymers include polysaccharides (e.g. starch, cellulose, pectin, etc.), proteins (e.g. caseinate, collagen, quinoa protein, etc.), extracts (e.g. beeswax, citrus extract, olive oil, *Silybum marianum* L. extract etc.). [66], [67], [77], [81], [82]

1.5 Thesis Outline and Objectives

Considering the overwhelming amount of waste resulting from tomato processing every year, the work developed in this master's thesis aims to valorize this raw material through the production and characterization of cutin monomers-enriched extracts. These extracts will be further used in the development and characterization of hydrophobic cutin-based films.

The thesis was structured in four different parts:

1. Extraction and depolymerization of cutin from tomato pomace.

2. Characterization of the monomeric cutin extracts obtained previously.

3. Production of cutin and chitosan-based films.

4. Characterization of the films regarding thickness, color, water contact angle and water vapor permeability.

2. Materials and Methods

2.1 Materials

Tomato Pomace

The tomato pomace used in this work (**Figure 2.1**) was kindly provided by SUMOL+COMPAL, S.A., specifically by the tomato paste manufacturing unit in Almeirim, Portugal. As soon as obtained, tomato pomace was packed into dark plastic bags and frozen at -20°C until the beginning of the experimental work.

Figure 2.1 - Sample of the thawed tomato pomace used in this work.

Reagents

Throughout the present work several reagents were used.

For the dewaxing of the tomato peels were used ethanol (99.9%, CARLO ERBA Reagents, Val de Reuil, France) and acetone (LABCHEM, Laborspirit, Lda., Loures, Portugal), or n-heptane (99.0%, CARLO ERBA Reagents, Val de Reuil, France). For the cutin depolymerization step, NaOH (pellets, eka, Laborspirit, Lda., Loures, Portugal) or KOH (pellets, eka, Laborspirit, Lda., Loures, Portugal), and for the isolation and purification of the cutin monomers, HCl (≥37%, Honeywell, Wien, Austria).

For the monomeric cutin extracts characterization were used methanol, sulfuric acid and chloroform (HPLC grade, Sigma-Aldrich, St. Louis, MO, USA).

For the chitosan filmogenic solution were used chitosan (Golden-Shell Biochemical Co., Ltd., Zhejiang, China), glacial acetic acid (99.8%, CARLO ERBA Reagents, Val de Reuil, France), and glycerol (≥99.0%, Sigma-Aldrich, Darmstadt, Germany). For the cutin solution were used ethanol (99.9%, CARLO ERBA Reagents, Val de Reuil, France) and Tween® 20 (≥40.0%, Sigma-Aldrich, St. Quentin Fallavier, France) or Tween® 80 (Sigma-Aldrich, St. Quentin Fallavier, France).

The water used in this work was purified using a Diwer Technologies purification unit, unless otherwise indicated.

Membranes

For the isolation and purification of cutin monomers, as an alternative method to precipitation, two polyethersulfone PES membranes (NADIR® NP010 P and NADIR® NP030 P, from MANN+HUMMEL Water & Fluid Solutions, Goleta CA, USA) were chosen (**Table 2.1**).

Table 2.1 - Characteristics of the membranes used in this study, according to the manufacturers' data.

Membrane	Material	MWCO[a] (Da)	pH range	Maximum pressure (bar)
NADIR® NP010 P	PES[b] on PP[c]	1000 – 1500	0.0 – 14.0	40
NADIR® NP030 P	PES[b] on PP[c]	500 – 1000	0.0 – 14.0	40

MWCO[a] – Molecular Weight Cut-Off; PES[b] – Polyethersulfone; PP[c] – Polypropylene.

2.2 Methods

2.2.1 Characterization of the Tomato Pomace

Determination of the Moisture Content

To determine the moisture content of the tomato pomace, 3 samples of approximately 10g of pomace were weighed and placed for a total of 120h (5 days) at 60°C in an oven (VENTICELL® 111 ECO line, MMM Group, Planegg, Germany). Samples were taken out from time to time and after the temperature dropped to room temperature its weight was registered. When a stabilization of the weight was achieved, i.e. no significant changes in the weight values (inferior to 0.01g), the moisture content (wet basis) – MC_{wb} – of the samples was determined using **Equation 2.1**.

$$MC_{wb} = \frac{m_{humid} - m_{dried}}{m_{humid}} \times 100 \qquad \textbf{(Equation 2.1)}$$

In this equation, m_{humid} refers to the mass of the humid tomato pomace and m_{dried} refers to the mass of the dried material.

Wet Separation of Tomato Peels

Tomato peels were separated from the other components of the tomato pomace, i.e. pulp, seeds and fibers. Samples of thawed tomato pomace were mixed with distilled water at room temperature of 20 times the sample weight in a small rectangular water tank (30 cm x 22 cm x 8 cm). The floating peels were recovered with a fine metallic mesh to drain off the water excess. The remaining mixture was stirred with a glass rod to allow peels that were dragged to the bottom of the water tank to float up and be recovered. The separation process was repeated several times until no more separation of peels was possible.

Drying and Milling Treatment

The tomato peels were dried in a hot air oven (VENTICELL® 111 ECO line, MMM Group, Planegg, Germany) for 48h at 60°C. This temperature was chosen to preserve the tomato peel components as much as possible. [36] Next, the dried tomato peels were milled into a fine flake form using an analytical grinder (A10 basic, IKA, Staufen, Germany) to increase the transfer area between the extracting solvent and the solid material.

2.2.2 Cutin Depolymerization and Extraction

Several methods were tested to depolymerize and consequently extract cutin from the tomato peels in this work. These were divided into three major groups. All these methods are summarized in **Figure 2.2**.

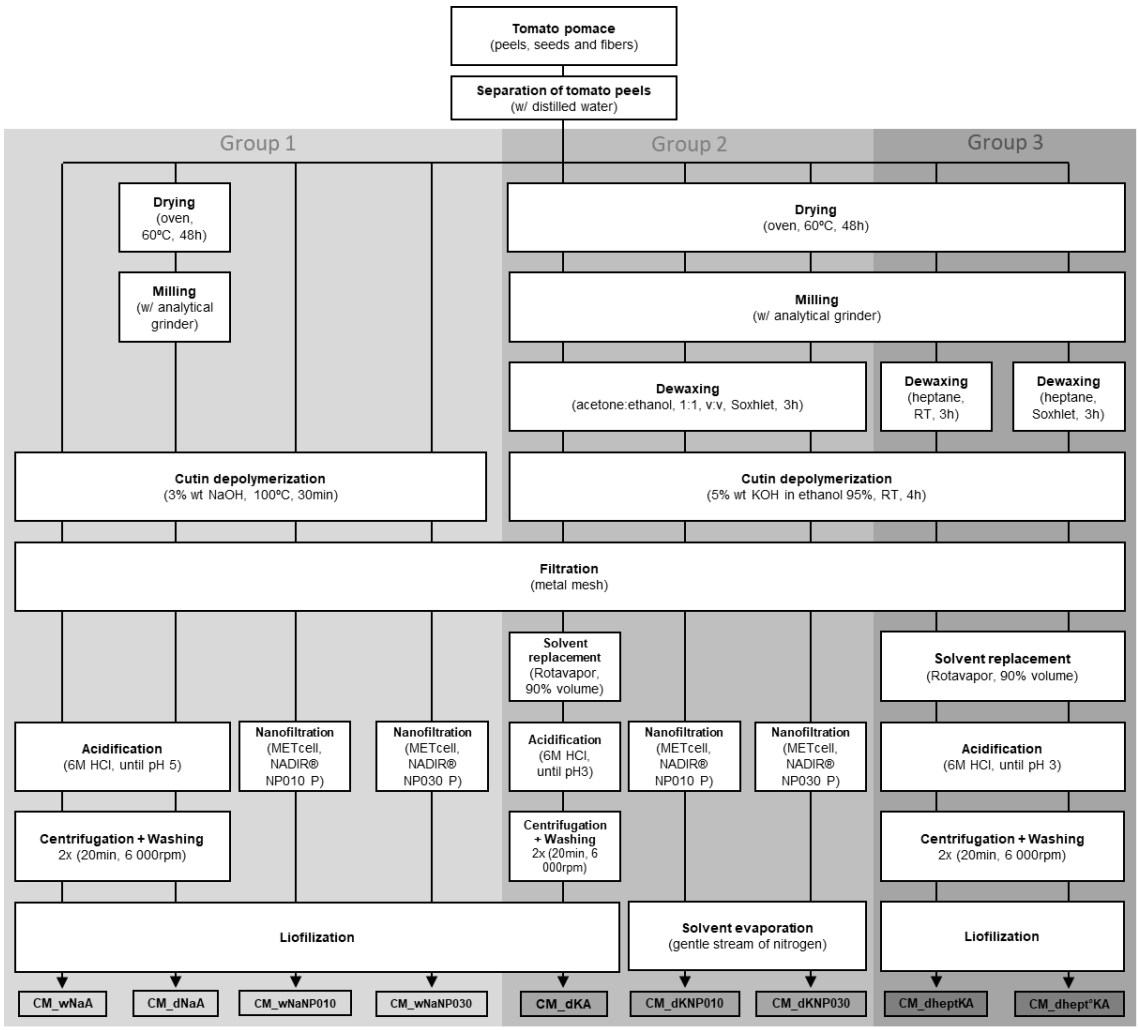

Legend:
w – wet tomato peels; **hept** – dewaxing with heptane (at RT); **Na** – alkaline hydrolysis with a NaOH solution; **A** – Acidification;
d – dried tomato peels; **hept°** – dewaxing with heptane (Soxhlet); **K** – alkaline hydrolysis with a KOH solution;
NP010 or **NP030** – Nanofiltration with a NADIR® NP010 P or NP030 P membrane;

Figure 2.2 - Flow diagram summarising all the methods tested in this study to depolymerize and extract cutin. In the figure, the legend refers to the nomenclature used to name the obtained monomeric cutin samples.

Group 1 – Alkaline Hydrolysis

The cutin depolymerization methods of the first group are based on the protocol previously described by Cigognini *et al.* [63], with some modifications. The tomato peels (thawed or dried and milled, see **Figure 2.2**) were mixed with a 3wt.% NaOH solution (NaOH solution/tomato peels ≈ 4/1, w/w). The mixture was then heated at 100°C for 30min by immersion on an oil bath (AREX Digital PRO, VELP® Scientifica, Usmate Velate (MB), Italy), under continuous stirring (300rpm). To remove spent skins, the produce was filtrated with a fine metallic mesh and the liquid fraction was collected. Cutin monomers were isolated and purified using one of two different methods - precipitation with an acidic solution or membrane processing (**Figure 2.2**).

Precipitation of cutin monomers was promoted by adjusting pH to 5 (SensION™+ pH3, Hach, Düsseldorf, Germany) with a 6M HCl solution. The extract enriched in cutin monomers was then recovered through centrifugation (Frontier™ Centrifuge FC5706, OHAUS, Zürich, Switzerland) of the suspension for 20min at 6 000rpm, washed twice with Milli-Q water and centrifuged likewise.

Alternatively, to precipitation, membrane filtration was performed in a MET®Cell Dead-End filtration system (Evonik Membrane Extraction Technology Ltd, London, UK), under constant pressure (10 bar), using flat sheet membranes (membrane area of 51.4cm^2.) (**Table 2.1**). During filtration, an electronic balance (Kern 572, KERN, Balingen, Germany) was used to measure permeate mass. For each filtration, a total of 100g of liquid extract enriched in cutin monomers were added to the system. The filtration process was conducted at room temperature under continuous stirring (400rpm). The extracts were processed until a final Volume Reduction Factor VRF [–] (the ratio between the initial feed volume and the retentate volume) of 3 was reached.

Samples resulting from both methods – acidification and membrane processing – were freeze-dried (48h treatment cycle) and then stored in a cold, dry and dark environment until further use and/or analyses.

Group 2 – Dewaxing (Acetone and Ethanol) and Ethanolic Alkaline Hydrolysis

The second group of cutin depolymerization methods followed the protocol previously described by Marc *et al.* [64], with some modifications. The dried and milled tomato peels (**Section 2.2.1 – Drying and Milling Treatment**) were dewaxed under the reflux of acetone: ethanol 1:1 (v/v) in a Soxhlet extractor. The extracting medium, i.e. the mixture of acetone and ethanol, was placed in a balloon, which was immersed in an oil bath (AREX Digital PRO, VELP® Scientifica, Usmate Velate (MB), Italy). A cellulose extraction thimble was filled with dried and milled tomato peels. The mass ratio of the extracting medium to dried and milled tomato peels was 23:1 and the time of extraction was 3h. Dewaxed tomato peels were dried overnight in a fume hood. For cutin depolymerization, the dewaxed tomato peels were mixed with 5wt.% KOH in ethanol 95% (KOH in ethanol solution/tomato peels ≈ 17/1, w/w). The depolymerization was performed at room temperature, with constant stirring at 300rpm, for 4h. To remove spent skins, the mixture was filtrated with a fine metallic mesh and the liquid fraction was collected. For three

methods, one from Group 2 and two from Group 3 (see **Figure 2.2**), about 90% of the filtrate's volume was evaporated under vacuum in a rotary evaporator (R-210, BUCHI®, Flawil, Switzerland) at 35°C and under reduced pressure (33 mbar). The volume evaporated was replaced by water. As in Group 1, isolation and purification of cutin monomers were achieved with precipitation with an acidic solution or membrane processing.

Precipitation of cutin was promoted by adjusting pH at 3.5 (SensION™+ pH3, Hach, Düsseldorf, Germany) with a 6M HCl solution. Cutin was then recovered through centrifugation of the suspension for 20 min at 6 000 rpm, washed twice with Milli-Q water and centrifuged likewise.

The membrane processing protocol was the same as for the methods in Group 1.

Samples resulting from both methods – acidification and membrane processing – were freeze-dried (48h treatment cycle) and then stored in a cold, dry and dark environment until further use and/or analyses.

Group 3 – Dewaxing (Heptane) and Ethanolic Alkaline Hydrolysis

The cutin depolymerization methods of Group 3 are very similar to those of Group 2, as can be seen in **Figure 2.2**, except for the dewaxing step. In Group 3, the dried and milled tomato peels were dewaxed with heptane. For one of the methods, the dewaxing was performed at room temperature, with constant stirring at 300rpm, for 3h. And for the other one dried and milled tomato peels were dewaxed under the reflux in a Soxhlet extractor. The extracting medium, i.e. heptane, was placed in a balloon, which was immersed in an oil bath (AREX Digital PRO, VELP® Scientifica, Usmate Velate (MB), Italy). A cellulose extraction thimble was filled with dried and milled tomato peels. The mass ratio of the extracting medium to dried and milled tomato peels was 23:1 and the time of extraction was 3h. Dewaxed tomato peels were dried overnight in a fume hood. Depolymerization was performed exactly as in Group 2 methods, as was isolation and purification of cutin monomers through precipitation with an acidic solution. No membrane processing was performed in this group of methods. The resulting samples were freeze-dried (48h treatment cycle) and then stored in a cold, dry and dark environment until further use and/or analyses.

Determination of the Extraction Yields

The extraction yield was calculated for each of the monomeric cutin extracts using **Equation 2.2**.

$$\text{Yield (\% w/w)} = \frac{m_{freeze-dried\ extract}}{m_{dried\ tomato\ peels}} \times 100 \qquad \textbf{(Equation 2.2)}$$

In this equation, $m_{freeze\text{-}dried\ extract}$ refers to the mass of the freeze-dried monomeric cutin extract and $m_{dried\ tomato\ peels}$ refers to the mass of the dried tomato peels from which the cutin has been extracted.

2.2.3 Characterization of the Monomeric Cutin Extracts (GC-FID)

The fatty acid content of the cutin monomer-enriched extracts was determined by GC-FID analysis at Laboratório de Análises, REQUIMTE-LAQV, Nova School of Sciences and Technology (Caparica, Portugal).

A first digestion step was performed following the method described by Lanham, *et al.* [83], with some modifications. Briefly, 2-4mg of each cutin lyophilized extract was incubated for methanolysis at 100°C, during 3.5h, with 1mL of acidic methanol (20% sulfuric acid) and 1mL of chloroform that contained nonadecanoic acid (1g/L) as internal standard (≥98%, Sigma-Aldrich, Darmstadt, Germany). After cooling, to separate the organic from the inorganic phase, 1mL of Milli-Q water was added and then vortex for 1min. The lower phases (organic phases) were extracted to GC vials of 2mL with molecular sieves to remove traces of water.

After the digestion step, the organic phase (methylated monomers dissolved in chloroform) of each sample was extracted and injected into a Gas Chromatograph coupled to a Flame Ionization Detector (GC-FID 6890, Agilent Technologies, Inc., Santa Clara, CA, USA and GC Autosampler HT3100A, HTA, Brescia, Italy). An OPTIMA 240 column (60m, 0.25mm ID and 0.25 µm film) (Macherey-Nagel, Duren, Germany), was used at a flow rate of 1.5mL/min. The mobile phase used was 33% cyanopropylmethyl - 67% dimethy polysiloxane. The oven temperature program was as follows: 80ºC; then 20ºC/min until 120ºC; and finally, 3ºC/min until 260ºC. The detector temperature was set at 280ºC. Palmitic acid (≥99%), stearic acid (≥98.5%), oleic acid (≥99%), linoleic acid (≥99%), 16-hydroxyhexadecanoic acid (98%), hexadecanedioic acid (98%) and octadecanedioic acid (98%) concentrations were determined using commercial (Sigma-Aldrich, Darmstadt, Germany) external standards (concentration range of 0.03125-1g/L) and corrected using a nonadecanoic acid as internal standard.

2.2.4 Preparation of Cutin and Chitosan Films

Preparation of the Films Solution/Suspension

The chitosan film-forming solution was prepared as described by Ferreira, A. R., *et al.* [84], with some modifications. Chitosan was dissolved in a glacial acetic acid solution (1% w/w), at a concentration of 1.5% w/w, and left stirring overnight at room temperature. Glycerol (25% $w_{glycerol}/w_{chitosan}$) was added to the solution, followed by another 20min of stirring for complete homogenization.

The monomeric cutin suspensions were prepared as previously described by Tedeschi, G., *et al.* [16], with some modifications. The selected extracts enriched in cutin monomers were added to a mixture of Milli-Q water and ethanol (1:1, v/v), at a concentration of 0.5% or 2% w/w, depending on the film sample. Tween® 80 or Tween® 20 (25% w_{Tween}/w_{cutin}) was added, and the mixtures were dispersed by successive ultrasound cycles using a 6mm diameter tapered microtip attached to a VCX750 ultrasonic processor (Sonics & Materials, Inc., Newtown, CT, USA).

Preparation of the Chitosan Films (control)

For the chitosan film (control), 10g of the chitosan solution was cast onto a 50mm diameter PFA evaporating dish (Bohlender, Grünsfeld, Germany) and dried overnight at 40°C in an oven (VENTICELL® 111 ECO line, MMM Group, Planegg, Germany). After being peeled from the dish, the film was stored and sealed in a glass petri dish and left in a desiccator at room temperature.

Preparation of Cutin and Chitosan Bilayer Films

A two-step coating technique was used to prepare the cutin and chitosan bilayer films. Primarily, 10g of the chitosan solution was cast onto the PFA evaporating dish (Bohlender, Grünsfeld, Germany) and then dried at 40°C in an oven (VENTICELL® 111 ECO line, MMM Group, Planegg, Germany) until it was obtained a firm but still adhesive surface. Then, 5g of the monomeric cutin suspension was cast on the top of the adhesive chitosan film and both layers were dried overnight in a 40°C oven (VENTICELL® 111 ECO line, MMM Group, Planegg, Germany). After being peeled from the PFA evaporating dishes, the films were stored and sealed in glass Petri dishes and left in a desiccator at room temperature.

Preparation of Cutin and Chitosan Blend Films

For the cutin and chitosan blend films, the monomeric cutin suspension was added to the chitosan solution (monomeric cutin suspension/chitosan solution ≈ 1/2, w/w) and the mixture was stirred for 20 min at room temperature until total homogenization. A mass of 15g of the cutin and chitosan solution was cast onto the PFA evaporating dish (Bohlender, Grünsfeld, Germany). These were then left to dry overnight in a 40°C oven (VENTICELL® 111 ECO line, MMM Group, Planegg, Germany). After being peeled from the PFA evaporating dishes, the films were stored and sealed in glass Petri dishes and left in a desiccator at room temperature.

All films produced are listed in **Table 2.2**, along with the strategy used (blend or bilayer), composition of the chitosan solution and the cutin monomer suspension, and ultrasonic dispersion program.

Table 2.2 - Summary of the strategy, composition of the chitosan solution and monomeric cutin suspension, as well as the ultrasonic dispersion program for each of the films produced.

Film sample	Strategy	Chitosan solution composition		Monomeric cutin suspension composition			
		Chitosan (w/w)	Glycerol ($w_{glycerol}/w_{chitosan}$)	Cutin monomers (w/w)	Tween® 80 (w_{Tween}/w_{cutin})	Tween® 20	Ultrasonic dispersion
(1)	-	1.5%	25%	-	-	-	-
(2)	Bilayer	1.5%	25%	2%	-	-	2x (1min, 20% amplitude)
(3)	Bilayer	1.5%	25%	2%	-	-	2x (1min, 20% amplitude) + 2x (1min, 30% amplitude)
(4)	Bilayer	1.5%	25%	0.5%	25%	-	3x (1min, 40% amplitude)
(5)	Bilayer	1.5%	25%	0.5%	-	25%	3x (1min, 40% amplitude)
(6)	Blend	1.5%	25%	0.5%	-	25%	3x (1min, 40% amplitude)
(7)	Blend	1.5%	25%	0.5%	-	25%	3x (1min, 40% amplitude)

2.2.5 Film Characterization

Before any of the following characterization procedures, the films were previously equilibrated at a relative humidity of 50.5% RH.

Thickness

To measure the thickness of the films, a digital micrometer (Filetta, Schut Geometrical Metrology, Groningen, Netherlands) was used. Measurements were made in three different places of the films.

Color Measurements

To assess the films in terms of color, the CIELAB (or CIE *L* a* b**) color system was chosen. [85] In order to calculate the exact values of a color, the *L* a* b** color system of the *Commission Internationale de l'Eclairage* (CIE) uses three axes – *L**, *a** and *b** – in a three-dimensional space (**Figure 2.3**). Parameter *L** measures lightness is usually represented in the vertical axis and its values range from 0 (black) to 100 (white). Parameters *a** and *b** measure the green/red and the blue/yellow color components, respectively. Negative values of *a** (-*a**) correspond to green and positive values (+*a**) correspond to red. The same happens for the

coordinate *b**, negative values of *b** (-*b**) correspond to blue and positive values (+*b**) correspond to yellow.

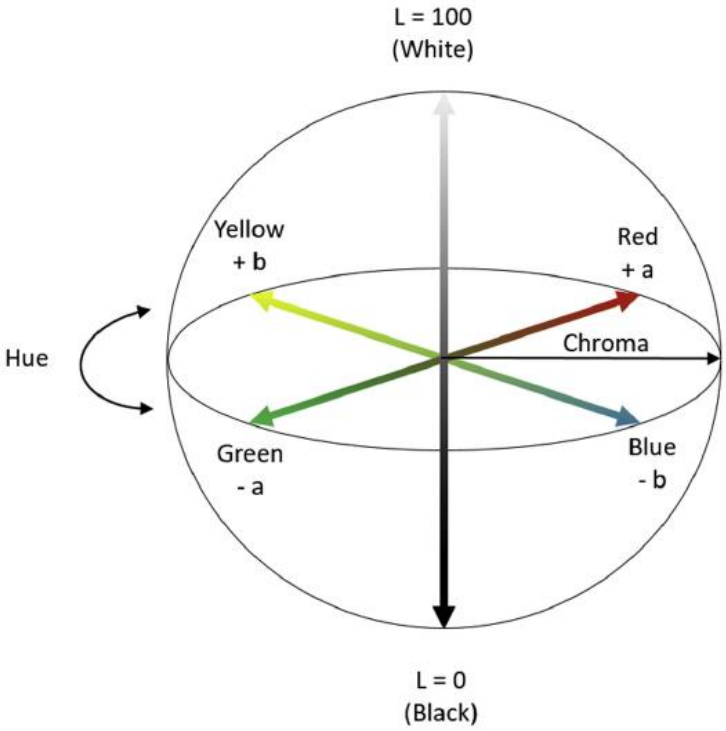

Figure 2.3 - The CIELAB color space diagram. [85]

A digital colorimeter (Chroma Meter CR-400, Konica Minolta, Tokyo, Japan) was used to obtain the values of these three parameters (*L**, *a** and *b**) for each of the selected films. First, the colorimeter was calibrated against a white calibration plate, where *L**= 94.52, *a**= -0.58 and *b**= 3.79. Following that, five measurements of different areas of the films (against the same white calibration plate) were performed.

By obtaining these values with the colorimeter, two other parameters can be and were calculated – the hue (*h*°) and the chroma (*C**). The hue represents the angle on the chromaticity axes and the chroma represents the distance from the central axis.

The *h*° was calculated using **Equation 2.3**:

$$h° = \arctan\left(\frac{b^*}{a^*}\right) \qquad \textbf{(Equation 2.3)}$$

Next, to convert the hue values from radians to degrees **Equations 2.4**, **2.5** or **2.6** were used:

$$h° = \arctan\left(\frac{b^*}{a^*}\right) \times \frac{180}{\pi}, \text{ for } a^* > 0 \text{ and } b^* > 0 \qquad \textbf{(Equation 2.4)}$$

$$h° = \left(\arctan\left(\frac{b^*}{a^*}\right) \times \frac{180}{\pi}\right) + 180, \text{ for } a^* < 0 \qquad \textbf{(Equation 2.5)}$$

$$h° = \left(\arctan\left(\frac{b^*}{a^*}\right) \times \frac{180}{\pi}\right) + 360, \text{ for } a^* > 0 \text{ and } b^* < 0 \qquad \textbf{(Equation 2.6)}$$

The *C** was calculated using **Equation 2.7**:

$$C^* = ((a^*)^2 + (b^*)^2)^{\frac{1}{2}} \quad \textbf{(Equation 2.7)}$$

In order to compare the color between each of the cutin and chitosan film samples and the control film sample (chitosan film), one more parameter was calculated – the color difference (ΔE^*_{ab}). The color difference considers the variation in the values of the parameters *L**, *a** and *b**, between two samples. It was calculated with **Equation 2.8**.

$$\Delta E^*_{ab} = ((\Delta L^*)^2 + (\Delta a^*)^2 + (\Delta b^*)^2)^{\frac{1}{2}} \quad \textbf{(Equation 2.8)}$$

If $\Delta E^*_{ab} > 1$ the color difference between the samples should be observable by the human eye. [85]

Water Contact Angle (WCA)

In order to determine the hydrophobicity of the films, water drop contact angles with their surfaces were measured. Water contact angle measurements were performed with the Drop Shape Analyser – DSA25 (KRÜSS, Hamburg, Germany), specifically using the Sessile Drop method. Using a microsyringe, a 3µL drop of distilled water was dropped onto the upper surface of previously cut squares of the film (1cm x 1cm). All measurements were performed at room temperature. Image analysis software ADVANCE (KRÜSS) was used to calculate the contact angles of the drops and the resulting values were given by the average on both sides of the drops. For each film type, three replicates were collected.

Water Vapor Permeability (WVP)

To evaluate the films in terms of their Water Vapor Permeability (WVP), a gravimetric method was chosen. The edges of the films were cut so that flat, smooth circular film samples were obtained. For this experiment, three film replicates were analyzed and, as already mentioned, all film samples were previously equilibrated at a relative humidity of 50.5% RH. These were sealed over cylindrical glass permeation cells with aluminum tape (**Figure 2.4**). The cylindrical glass cells (inner diameter = 40mm) were previously filled with 9mL of a saturated NaCl solution (a_w = 0.755).

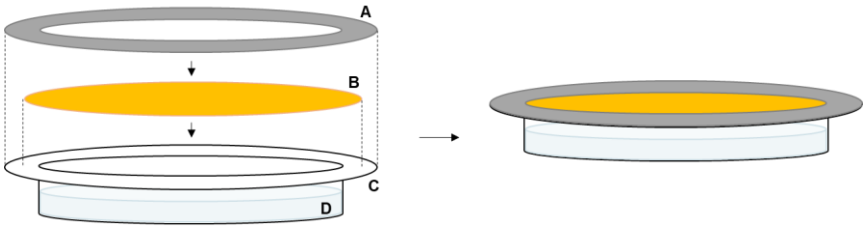

Figure 2.4 - Schematic representation of the film disposal in the cylindrical glass cell during the WVP assay. A – Aluminum tape; B – Film sample; C - Cylindrical glass permeation cell; D - Saturated NaCl solution.

After this, each of the permeation sets (1 permeation set = cylindrical glass cell + NaCl solution + film sample + aluminum tape) was quickly weighed. Then all of the sets were put in a desiccator containing a saturated $MgCl_2$ solution (a_w = 0.328) and equipped with a fan to promote air circulation (**Figure 2.5**). The permeation sets were weighed at regular time intervals for eight hours. During each of these weighings, the temperature and relative humidity inside the desiccator were measured with a thermohygrometer (HUMICAP® HM40, Vaisala, Helsinki, Finland).

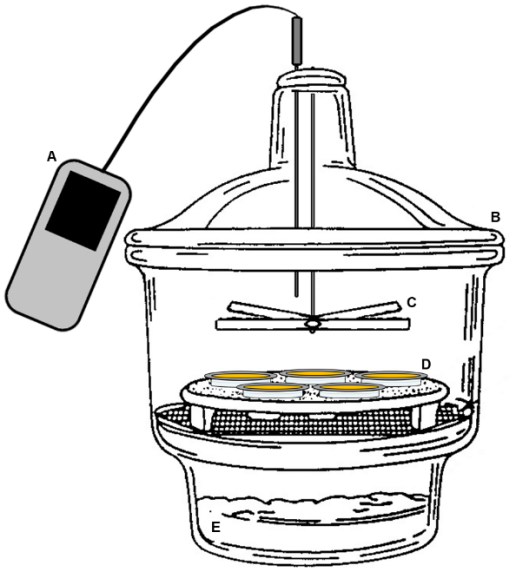

Figure 2.5 - Representative diagram of the setup created for the WVP experimental assay. A – Thermohygrometer; B – Desiccator; C – Fan; D – Permeation sets (cylindrical glass cell + NaCl solution + film sample + aluminum tape); E – Saturated $MgCl_2$ solution.

The WVP was calculated using **Equation 2.9**:

$$\mathrm{WVP} = \frac{N_w \times \delta}{\Delta P_{w.eff}} \qquad \textbf{(Equation 2.9)}$$

In this Equation, N_w (mol/m^2.s) is the water vapor flux, δ (m) is the film thickness and $\Delta_{Pw.eff}$ (Pa) is the effective driving force. To calculate N_w, the slope of the plot of the mass of water evaporated from the permeation sets over time (mol/s) was divided by the exposed area of the film (m^2).

The $\Delta_{Pw.eff}$ was calculated using **Equation 2.10**:

$$\Delta P_{w.eff} = P_{w2} - P_{w3} \qquad \textbf{(Equation 2.10)}$$

For this, P_{w2} was calculated using **Equation 2.11**:

$$P_{w2} = P - (P - P_{w1}) \times exp\left[\frac{N_w RTz}{P\ D_{w-air}}\right] \qquad \textbf{(Equation 2.11)}$$

In this Equation, P (Pa) is the atmospheric pressure and P_{w1} (Pa) is the water partial pressure in contact with the solution in the glass permeation cells. R (J.K^{-1}mol^{-1}) is the gas constant, T (K) is

the mean temperature, z (m) is the distance from the film to the solution in the cylindrical glass permeation cell and $D_{w\text{-}air}$ ($m^2.s^{-1}$) is the water vapor diffusion coefficient in air.

The P_{w1} was calculated using **Equation 2.12**:

$$P_{w1} = P_w^* \times a_w \qquad \textbf{(Equation 2.12)}$$

In this Equation, P^*_w (Pa) is the pure water vapor pressure and a_w is the water activity of the saturated NaCl solution in the interior of the cylindrical glass permeation cells.

The P^*_w was calculated using **Equation 2.13**:

$$P_w^* = exp\left(23.1964 - \frac{3816.44}{T-46.13}\right) \qquad \textbf{(Equation 2.13)}$$

The P_{w3} (in Equation 2.10) was calculated using **Equation 2.14**:

$$P_{w3} = \frac{RH \times P_w^*}{100} \qquad \textbf{(Equation 2.14)}$$

In this Equation, RH (%) is the average of the values of relative humidity measured.

3. Results and Discussion

Preliminary analyses to determine the general composition/physical characteristics of the tomato pomace residue were conducted.

3.1 Tomato Pomace

3.1.1 Moisture Content

In a first approach, the residue was dried to gravimetrically determine its moisture content value (**Table 3.1**).

Table 3.1 - Moisture content value determined for the tomato pomace used in the present work. Results are given as % ($w_{water}/w_{humid\ tomato\ pomace}$).

	Moisture content (wet basis), % ($w_{water}/w_{humid\ tomato\ pomace}$)
Tomato pomace	84.07 ± 0.42

It is challenging to compare the moisture content value obtained with those reported in the literature (**Section 1.2.1** of this thesis – **Table 1.1**) since the reported ranges are so wide. Nevertheless, the batch of tomato pomace used in this study showed an undeniable high value of water content. This value is very similar to the one obtained by Bhat and Ahsan [31], whose batch of fresh tomato pomace presented a moisture content of 87.63 ± 0.12% (w/w).

Such high values of water content make tomato pomace a highly perishable material, susceptible to microbial degradation. In light of this information, it was decided to freeze the pomace until further use. Other preservation methods, such as freeze-drying [31], could also have been applied to prevent pomace spoilage during the research. Nevertheless, freezing was the most logical method given the next steps in the study.

3.1.2 Peel, Seed and Fiber

The separation results of the dried tomato pomace into fractions – skins, seeds and fibers – are shown in **Figure 3.1** and their corresponding numerical values are listed in **Table 3.2**.

Figura 3.1 - Peels, seeds and fibers (left to right) from dried tomato pomace, manually separated.

Table 3.2 - Peel, seed and fiber ratio values determined for the batch of tomato pomace used in the present work. Results are given as % ($w_{dried\ component}/w_{dried\ tomato\ pomace}$).

Fraction	**Dried component,** % ($w_{dried\ component}/w_{dried\ tomato\ pomace}$)
Peel	63.62 ± 1.85
Seed	34.59 ± 2.51
Fiber	1.80 ± 0.73

The obtained values suggest that peels correspond to the largest fraction of the tomato pomace studied in this work, accounting for more than half of its dry weight. Seeds account for just over a third, and fibers, in less quantity, not reaching 2% (w/w).
In **Table 3.2**, the fraction with the highest content in dried matter was the peel fraction, which is in line with the results reported in **Section 1.2.1** of this thesis (**Table 1.2**).

Prior to cutin depolymerization procedures, a fast and simple sedimentation process to separate the pomace into its peel and seed fractions was carried out. This aimed to obtain extracts with a higher cutin concentration since cutin is part of the tomato's cuticle, which is a constituent element of the tomato peel, as previously mentioned.

3.2 Tomato Monomeric Cutin Extracts

Images of all the monomeric cutin extracts produced are shown in **Table 3.3**.

Table 3.3 - Appearance of monomeric cutin extracts from tomato peels.

Group	**Group 1**			
Sample	**CM_wNaA**	**CM_dNaA**	**CM_wNaNP010**	**CM_wNaNP030**
Appearance of the monomeric cutin extract	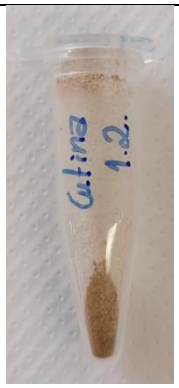	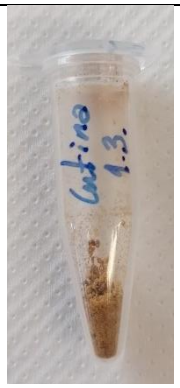	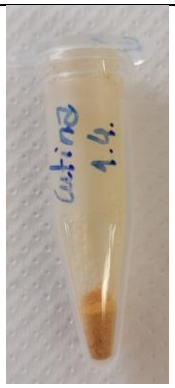	

Group	**Group 2**			**Group 3**	
Sample	**CM_dKA**	**CM_dKNP010**	**CM_dKNP030**	**CM_dheptKA**	**CM_dheptºKA**
Appearance of the monomeric cutin extract		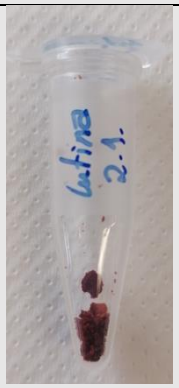			

Note: The mass of extracts that can be visualized in the images is not representative of the total mass of extract obtained.

Each of the monomer-enriched cutin extracts was designated according to their extraction method. All sample identifications begins with "CM" referring to cutin monomers, followed by the raw material's state with which the extraction was initiated – "**w**" for wet tomato peels or "**d**" for dried tomato peels. The alkaline solution used for cutin depolymerization was identified in the samples designation with "**Na**" for samples which tomato peels were hydrolyzed with an aqueous sodium hydroxide solution or "**K**" for samples whose hydrolysis was performed with an ethanolic solution of potassium hydroxide. The samples whose isolation and purification of cutin monomers was accomplished by precipitation with an acidic solution were attributed the nomenclature "**A**" or, alternatively, "**NP010**" or "**NP030**" if this step was performed by nanofiltration with an NADIR® NP010 P or NADIR® NP030 P membrane, respectively. The nomenclature "**hept**" or "**heptº**" refers to samples for which the dewaxing step was performed with heptane at room temperature or under reflux in a Soxhlet extractor, respectively.

In light of this, the monomeric cutin sample CM_wNaA was obtained by alkaline hydrolysis of the wet tomato peels with an aqueous sodium hydroxide solution. This was followed by precipitation of the cutin monomers with a concentrated hydrochloric acid solution. The extraction method that resulted in sample CM_dNaA differs from the first only in the use of dried and milled rather than wet tomato peels.

Samples CM_wNaNP010 and CM_wNaNP030 were produced by the same extraction method used to produce sample CM_wNaA up to the cutin monomers isolation step. In the case of the first two samples this isolation was performed by membrane processing rather than by precipitation with an acid solution. The extraction methods that led to the production of samples CM_dKA, CM_dKNP010 and CM_dKNP030 started with the dewaxing of dried and milled tomato peels with a mixture of acetone and ethanol under reflux in a soxhlet extractor, followed by cutin depolymerization through alkaline hydrolysis with an ethanolic solution of potassium hydroxide. The difference between the methods arises in the monomer isolation step, which for sample CM_dKA was by acidification and for samples CM_dKNP010 and CM_dKNP030 was by nanofiltration.

The extraction methods that resulted in samples CM_dheptKA and CM_dheptºKA differ from the extraction method of sample CM_dKA only in the solvent used for removing waxes from the tomato peels. For the first two samples was used heptane and for the latter was used a mixture of acetone and ethanol.

The cutin extraction methods produced extracts with very different colors and textures. Samples CM_wNaA and CM_dNaA (Group 1) dried into a light brownish-orange crystalline solid. Samples CM_wNaNP010, CM_wNaNP030 (Group 1) and CM_dKA (Group 2), on the other hand, presented a yellowish-orange tone. The texture of samples CM_wNaNP010 and CM_dKA being of a crystalline solid and sample CM_wNaNP030 of a grainy sticky mass. Samples CM_dKNP010 and CM_dKNP030 (Group 2), and samples CM_dheptKA and CM_dheptºKA (Group 3) dried into much darker red and brown solids, with grainy sticky mass (CM_dKNP010 and CM_dKNP030) and flaky (CM_dheptKA and CM_dheptºKA) textures.

3.2.1 Monomeric Cutin Extraction Yields

The extraction yield value was calculated for each of the monomer-enriched cutin extracts produced (**Table 3.4**).

Table 3.4 - Extraction yields of monomeric cutin from tomato peels. Results are given as % ($w_{freeze\text{-}dried\ extract}/w_{dried\ tomato\ peels}$).

	Group 1				Group 2			Group 3	
	CM_ wNaA	**CM_ dNaA**	**CM_ wNaNP010**	**CM_ wNaNP030**	**CM_ dKA**	**CM_ dKNP010**	**CM_ dKNP030**	**CM_ dheptKA**	**CM_ dheptºKA**
Extraction yield, % (w/w)	6.74	16.46	38.83	28.48	21.11	88.16	82.00	26.64	19.17

Cutin extraction methods investigated showed significant differences in terms of extraction yield.

By comparing extraction yield values of samples CM_wNaA and CM_dNaA (Group 1), one can infer that the sample in which tomato peels were dried and milled prior to cutin depolymerization – sample CM_dNaA – had the highest yield. This may suggest that the efficiency of the depolymerization reaction is influenced by the moisture content of the material soon to be hydrolyzed and the surface area between the solvent and the solid material.

The extraction yields of the methods using membrane separation processes for monomeric cutin isolation (which resulted in samples CM_wNaNP010 and CM_wNaNP030 from Group 1 and samples CM_dKNP010 and CM_dKNP030 from Group 2) were overall higher than the acidification corresponding ones (sample CM_wNaA from Group 1 and sample CM_dKA from Group 2). Less pure cutin extracts may have been obtained with the membrane processing technology. As is known, this method is based on the separation of molecules according to their molecular weight, in contrast to acidification, which favors the precipitation of compounds according to their chemical composition and ionic charge. It is possible that, in this specific case, acidification was the most selective method, something that can only be deduced with more certainty with the analysis of the composition of the extracts.

Samples CM_dheptKA and CM_dheptºKA from Group 3 had comparable yield values to that obtained for sample CM_dKA from Group 2, with the value of sample CM_dheptKA being slightly higher. However, to possibly compare the efficiency of the solvent (mixture of water and ethanol in Group 2 *versus* heptane in Group 3) in removing the waxes from tomato peels more tests should be performed.

Cigognini *et al.* [63] reported a 15% (w/w) yield value for the method used in this work to produce sample CM_wNaA, for which a lower value of 6.74% (w/w) was obtained. This difference may be due to either the time or the temperature values chosen for the depolymerization reaction, or more likely both. In this work the reaction was run for 30min at 100ºC, while the authors let the reaction run for 2h without specifying the temperature used, giving only a range.

The extraction yield value of sample CM_dKA was 21.11% (w/w), significantly lower than the 60% (w/w) obtained by Marc *et al.* [64]. However, this difference can be directly related to the reaction time of the depolymerization step. While Marc *et al.* [64] left the reaction running for 24h, in this study only the effect of 4h of depolymerization was studied.

Despite this, ethanolic alkaline hydrolysis at room temperature (sample CM_dKA) led to a higher yield of monomeric cutin extract than that for aqueous alkaline hydrolysis at 100°C (samples CM_wNaA and CM_dNaA), which may be a very interesting finding in terms of process sustainability.

3.2.2 Fatty Acid Composition

The results of the fatty acid composition of the monomeric cutin extracts, investigated by GC-FID, are presented in **Table 3.5.** (results given as % ($w_{fatty\ acid}/w_{total\ fatty\ acids}$)) and **Table 3.6.** (results given as % ($w_{fatty\ acid}/w_{freeze\text{-}dried\ extract}$)).

Table 3.5 - GC-FID analysis of the constituents identified in cutin samples. Results are given as % ($w_{fatty\ acid}/w_{total\ fatty\ acids}$).

	Group 1				Group 2			Group 3	
Fatty acid	**CM_ wNaA**	**CM_ dNaA**	**CM_ wNaNP010**	**CM_ wNaNP030**	**CM_ dKA**	**CM_ dKNP010**	**CM_ dKNP030**	**CM_ dheptKA**	**CM_ dheptºKA**
Palmitic acid	14.47	31.04	12.26	12.27	6.33	11.52	11.85	10.74	-
Stearic acid	10.44	14.32	16.30	16.62	5.61	13.07	13.57	7.45	-
Oleic acid	6.31	10.71	7.87	7.84	2.82	6.91	7.07	4.61	-
Linoleic acid	16.29	11.97	12.94	12.41	7.22	12.71	12.54	12.68	-
Hexadecanedioic acid	17.54	15.41	15.53	14.81	10.51	14.61	15.08	13.38	-
16-hydroxy-hexadecanoic acid	23.66	8.07	20.67	21.64	62.05	28.48	26.70	43.41	-
Octadecanedioic acid	11.30	8.49	14.43	14.41	5.46	12.70	13.19	7.73	-

Table 3.6 - GC-FID analysis of the constituents identified in cutin samples. Results are given as % ($w_{fatty\ acid}/w_{freeze\text{-}dried\ extract}$).

	Group 1				Group 2			Group 3	
Fatty acid	**CM_ wNaA**	**CM_ dNaA**	**CM_ wNaNP010**	**CM_ wNaNP030**	**CM_ dKA**	**CM_ dKNP010**	**CM_ dKNP030**	**CM_ dheptKA**	**CM_ dheptºKA**
Palmitic acid	1.86	6.55	0.80	0.78	1.71	1.21	1.01	1.96	-
Stearic acid	1.34	3.02	1.06	1.05	1.52	1.37	1.15	1.36	-
Oleic acid	0.81	2.26	0.51	0.50	0.76	0.72	0.60	0.84	-
Linoleic acid	2.09	2.53	0.84	0.79	1.95	1.33	1.07	2.31	-
Hexadecanedioic acid	2.25	3.25	1.01	0.94	2.84	1.53	1.28	2.44	-
16-hydroxy-hexadecanoic acid	3.03	1.70	1.35	1.37	16.76	2.99	2.27	7.90	-
Octadecanedioic acid	1.45	1.79	0.94	0.91	1.47	1.33	1.12	1.41	-
Total fatty acids	6.07	24.71	4.11	4.19	8.22	4.68	4.41	6.97	

Considering the results presented in **Table 3.5**, the major fatty acid identified was 16-hydroxyhexadecanoic acid, with the highest percentage ($w_{fatty\ acid}/w_{total\ fatty\ acids}$) in seven out of the eight samples analyzed, ranging from 62.05% in sample CM_dKA to 8.07% in sample CM_dNaA. Followed by hexadecanedioic acid, the second major fatty acid in six out of the eight samples, with a range of values from 17.54% (sample CM_wNaA) to 10.51% (sample CM_dKA). Stearic, linoleic, palmitic and octadecanedioic acids have also been identified, although in smaller amounts than the previous fatty acids. The component with the lowest percentage ($w_{fatty\ acid}/w_{total\ fatty\ acids}$), in seven out of the eight samples analyzed, was oleic acid, ranging from 10.71% in sample CM_dNaA to 2.82% in sample CM_dKA.

On a more thorough level and analyzing samples that are within the same group there are also some observations that can be drawn. When comparing samples CM_wNaA and CM_dNaA (Group 1), whose difference in the extraction method is based on the use of humid tomato peels (sample CM_wNaA) or dried and milled tomato peels (sample CM_dNaA), it is evident that there are differences in the fatty acid profile of the two samples. Although the second major component, hexadecanedioic acid, was the same for both samples, representing 17.54% of the total fatty acids investigated in sample CM_wNaA and 15.41% in sample CM_dNaA, that was not the case for the most predominant compound. The major fatty acid identified in sample CM_wNaA was 16-hydroxy-hexadecanoic with a total percentage of 23.66%. In sample CM_dNaA, on the other hand, it was palmitic acid representing 31.04% of total fatty acids.
Therefore, it is possible that the drying and milling pretreatment of tomato peels may be an influencing factor on the final fatty acid profile. In the sense that the existence of this pretreatment may contribute to more or less complete depolymerization of cutin.

Also, within Group 1, for samples CM_wNaNP010 and CM_wNaNP030, very similar fatty acid profiles were obtained. It should be noted that the only difference between the extraction methods that originated the two samples was the use of a membrane with a smaller pore size in the case of sample CM_wNaNP030 (MWCO of 500 – 1000Da) and larger pore size in the case of sample CM_wNaNP010 (MWCO of 1000 – 1500Da). This may indicate that the membrane processing step was not efficient in isolating the cutin monomers. Combining the cutin extraction yield values (**Table 3.4**) with the fatty acid profiles further supports this hypothesis. Samples CM_wNaNP010 and CM_wNaNP030 have extraction yields of 38.83 and 28.48% ($w_{freeze\text{-}dried\ extract}/w_{dried\ residue}$), respectively, while sample CM_wNaA has a yield value of 6.74%. However, samples CM_wNaNP010 and CM_wNaNP030 do not show a higher weight percentage of fatty acids per weight of freeze-dried extract (**Table 3.6**). Thus, this supports what was previously indicated in the previous section (**Section 3.2.1**), suggesting that the membrane processing step was not more efficient when compared to the alternative method of cutin monomer isolation - precipitation with an acidic solution (sample CM_wNaA).
This can also be observed with samples from Group 2. Samples CM_dKNP010 and CM_dKNP030 had extraction yield values that were four times higher than that of CM_dKA. However, these values do not translate into higher values of fatty acid concentration.

Unfortunately, it was not possible to investigate the presence of the fatty acid reported as the most predominant in monomeric cutin extracts (10,16-dihydroxyhexadecanoic acid) owing to the impossibility of acquiring this standard. However, in future studies, it is intended to evaluate the extracts accordingly. Nevertheless, to a certain extent, these results are in agreement with those reported in **Section 1.4.1** of this thesis, in the sense that the presence of many of the same compounds was detected in the extracts produced, namely 16-hydroxy-hexadecanoic acid, linoleic acid, oleic acid, palmitic acid, etc.

The samples selected for the study of the cutin-based film production were the samples CM_dNaA (Group 1) and CM_dKA (Group 2), because these samples had the highest mass percentage of total fatty acid per mass of freeze-dried extract.

3.3 Cutin and Chitosan Films

After successfully obtaining monomeric cutin extracts, their applicability in the production of hydrophobic films was studied.

Films with cutin were developed together with a polysacharide, two important compounds in the structure of natural cuticle in tomato peels. Specifically, the polysacharide chitosan was selected due to its excellent biocompatibility, biodegradability, film-forming and antimicrobial properties commonly reported in literature. [77]–[79], [82]

All films were produced by the casting method and are shown in **Table 3.7**.

Film sample (1) resulted from the casting of a solution of chitosan dissolved in acetic acid (1.5% w/w), containing glycerol as platicizer.

Film samples (2) and (3) were produced from a double-layer strategy in which the bottom layer of the films was obtained by pre-drying a chitosan film-forming solution – with the same formulation as that of film sample (1) –, followed by the addition and drying of a monomeric cutin suspension on top of the chitosan layer. This suspension was produced by dispersing monomers of the CM_dKA cutin extract in a mixture of water and ethanol (2.0% w/w).

Film samples (4) and (5) were produced with the same strategy as the previous samples, the difference being in the composition of the monomeric cutin suspensions. The suspensions of these films had a concentration of cutin monomers of 0.5% w/w and contained Tween® 20 or Tween® 80 as dispersing agents.

Finally, film samples (6) and (7) were produced by drying the blend of a 1.5% w/w chitosan solution with a suspension of cutin monomers – monomeric cutin extract CM_dKA or CM_dNaA in water and ethanol, and containing the dispersing agent Tween® 20.

After being removed from the oven, where the films dried at 40°C overnight, all films were easily peeled from the PFA evaporating dishes.

Table 3.7 - Composition of film-forming solution and respective resulting film appearance of all the films produced in this work.

Identification/composition of the film	Appearance of the film
(1) 1.5% Chitosan (control)	

(2) 1.5% Chitosan + 2.0% Cutin CM_dKA (bilayer)	
(3) 1.5% Chitosan + 2.0% Cutin CM_dKA (bilayer)	
(4) 1.5% Chitosan + 0.5% Cutin CM_dKA + Tween® 80 (bilayer)	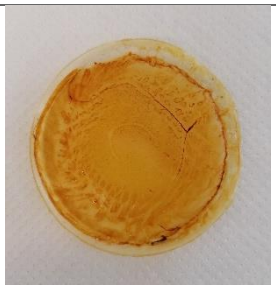
(5) 1.5% Chitosan + 0.5% Cutin CM_dKA + Tween® 20 (bilayer)	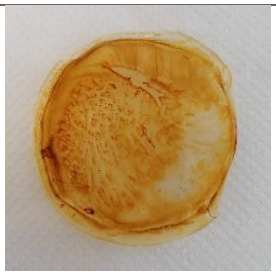
(6) 1.5% Chitosan + 0.5% Cutin CM_dKA + Tween® 20 (blend)	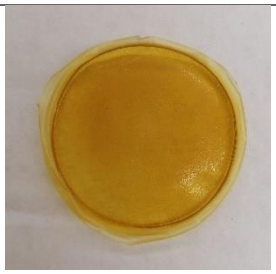
(7) 1.5% Chitosan + 0.5% Cutin CM_dNaA + Tween® 20 (blend)	

The chitosan films produced – **Table 3.7**, film sample (1) – were homogeneous, flexible and very easy to handle. Visually, these films appeared to be transparent with a slightly yellowish coloration.

Cutin and chitosan films – **Table 3.7**, film samples (2) to (7) – displayed an orange to red range of colors, as a result of adding the cutin extracts (**Table 3.3**) to the solution or film of chitosan.

Bilayer film samples (2) and (3) were significantly less malleable when compared to the chitosan control film. The upper surface (cutin layer) had a very rough texture, and the films were visually heterogeneous. These results may have occurred due to an excessive concentration of monomeric cutin in the suspensions, in combination with a poor dispersion of these suspensions. Although both suspensions of cutin monomers appeared to be well dispersed, the non-uniformity of the upper surface of the bilayer film samples (2) and (3) show otherwise and suggest that during the drying step of the films there was an aggregation of the suspension components, resulting in the heterogeneous films that the images show.

Given these results, some adjustments were made to the composition of the cutin monomer suspension for the production of the following films. Specifically, a decrease of the concentration of cutin monomers in the solution, from 2 to 0.5% (w/w), an increase in the time and amplitude of the ultrasound dispersion cycles, and the addition of surfactants such as Tween® 20 and Tween® 80. The addition of these surfactants to the suspensions emerges in an attempt to stabilize the emulsions for improving the separation of the particles and preventing their aggregation. The result of these adjustments is reflected in bilayer film samples (4) and (5).

Film samples (4) and (5) were more malleable than the previous ones and had a much more smooth, less rough upper surface texture, but were still not homogeneous and non-uniform by naked eye observation. For these reasons, the characterization of these films was not performed.

Finally, blend films (6) and (7) of cutin and chitosan were produced, and were the most malleable and the most homogeneous. Therefore, film samples (6) and (7) proceeded to the next stage of characterization. Even so, when comparing both, film (6) had the smoothest, most uniform and homogeneous surface detectable to the naked eye (**Figure 3.2**). It is very likely that these observable differences in the two film samples are due to the monomeric cutin extracts that each of these films have in their composition. Differences between the two cutin extraction methods that originated CM_dNaA and CM_dKA extracts, such as the existence of a dewaxing step, the type of alkaline solution and the temperature at which the depolymerization of the cutin occurred, most likely contributed to obtaining different monomeric cutin extracts and, consequently, resulting in films with different appearances.

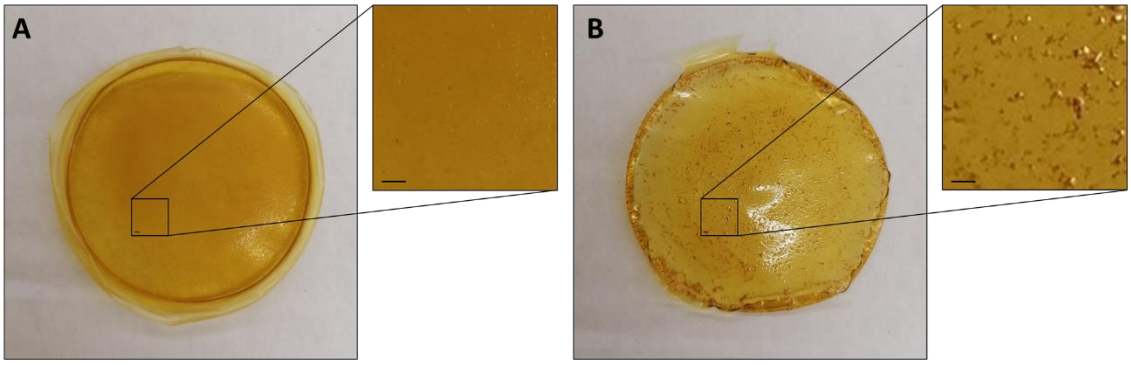

Figure 3.2 - Cutin and chitosan-based blend films. A – Film sample (6) - 1.5% Chitosan + 0.5% Cutin CM_dKA + Tween® 20. B – 1.5% Chitosan + 0.5% Cutin CM_dNaA + Tween® 20. Scale bar = 1mm.

3.3.1 Characterization of Cutin and Chitosan Films

The chitosan-based film and the two selected cutin and chitosan-based blend films in the previous section were characterized in terms of thickness, color, water contact angle and water vapor permeability.

Thickness

The thickness values of the films are listed in **Table 3.8**.

Table 3.8 - Thickness (mm) of the selected film samples.

Film samples	Thickness (mm)
(1) 1.5% Chitosan (control)	0.092 ± 0.008
(6) 1.5% Chitosan + 0.5% Cutin CM_dKA + Tween® 20 (blend)	0.103 ± 0.004
(7) 1.5% Chitosan + 0.5% Cutin CM_dNaA + Tween® 20 (blend)	0.106 ± 0.005

The chitosan film (control) – film sample (1) – presented the lowest thickness value, being the thinnest film produced in this work, with an average thickness of 0.092 ± 0.008mm. Cutin and chitosan film samples (6) and (7) showed slightly higher thickness values, respectively, 0.103 ± 0.004 and 0.106 ± 0.005mm.

These results were as expected since the cutin and chitosan films were produced to have the same mass of chitosan film-forming solution as the control film, i.e. 10g of chitosan filmogenic solution. Therefore, the difference in thickness between these films and the control should be mostly due to the non-volatile matter of the monomeric cutin suspensions added. Additionally, it was also anticipated that the thickness value of film sample (6) would be very close to that of film sample (7) since the only difference in the composition of the two films is the depolymerized cutin extract used. For the production of film sample (6) the monomeric cutin extract used was CM_dKA and for film sample (7) was CM_dNaA.

Color

The exact colors of the films were determined according to the CIELAB color system. The measured (*L**, *a** and *b**) and the calculated (*h°* and *C**) color parameters are summarized in **Table 3.9**.

Table 3.9 - Measured color parameter values: lightness (L*), chromaticity coordinates (a* and b*) and their respective calculated hue (hº) and chroma (C*) of the selected film samples.

Film samples	*L**	*a**	*b**	*h°*	*C**
(1) 1.5% Chitosan (control)	92.72 ± 0.77	-1.99 ± 0.29	10.50 ± 1.47	100.72 ± 0.19	10.68 ± 1.49
(6) 1.5% Chitosan + 0.5% Cutin CM_dKA + Tween® 20 (blend)	72.18 ± 2.43	4.99 ± 2.13	55.63 ± 0.69	84.86 ± 2.25	55.89 ± 0.52
(7) 1.5% Chitosan + 0.5% Cutin CM_dNaA + Tween® 20 (blend)	76.38 ± 0.95	2.52 ± 0.79	49.58 ± 1.42	87.10 ± 0.83	49.65 ± 1.45

For the chitosan control film sample (1), a very high lightness (*L**) value was obtained (92.72). This value was very close to 100 (white) and, therefore, very far from 0 (black), indicating that the film had a very light shade. As for the *a** and *b** coordinates, this film presented a negative *a** value (-1.99) and a positive *b** value (10.50), resulting in a h^o value of 100.72 and a *C** value of 10.68. These values confirm what was observed with the naked eye, i.e. that the films had a yellowish tone with a low color saturation.

These color results for the chitosan-based films match those produced by Leceta *et al.* [79], especially the films produced with low molecular weight (LMw) chitosan and 30% $w_{glycerol}/w_{chitosan}$.

The color parameters of cutin and chitosan film samples (6) and (7) varied, as expected, from the chitosan control film. Both samples, (6) and (7), had lower *L** values, which is consistent with the film's darker colors observed visually. Unlike the control film, these two samples showed positive values of the *a** coordinate, which indicates a color transition from green to red tones, completely expected given that orange/red extracts of depolymerized cutin were added to the chitosan film-forming solutions for the production of these films. On the other hand, the control film and the samples both revealed positive *b** coordinates, but significantly higher values in the cutin and chitosan samples, indicating that these films have a more intense yellow color component. These differences in a* and b* coordinate values resulted in lower h^o values for the (6) and (7) samples. Finally, higher chroma (*C**) values were obtained for the cutin and chitosan film samples, mirroring the increase in color saturation that could be observed when comparing these to the control film.

By obtaining these color parameters, in particular the *a** and *b** chromaticity coordinates, it was possible to determine the approximate color position of these films in the CIELAB hue circle (**Figure 3.3**).

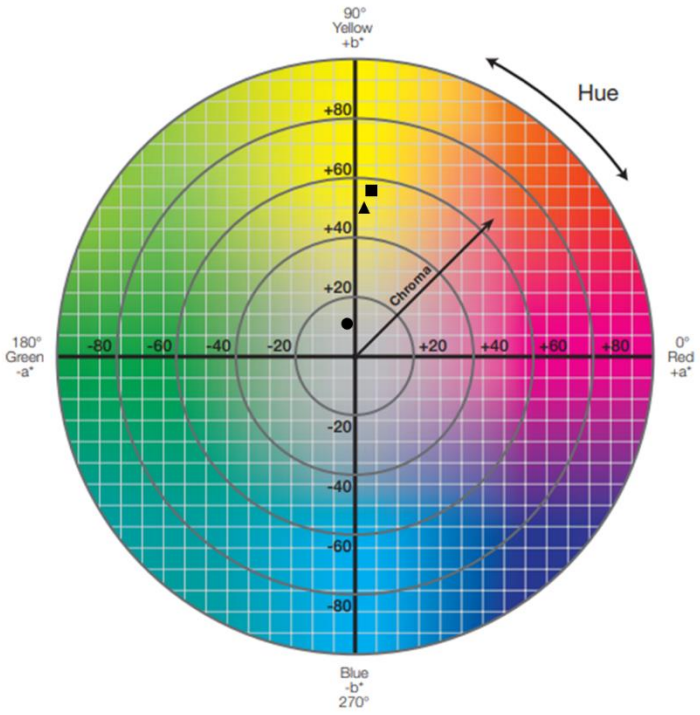

Figure 3.3 - Graphic representation of the color of the three films, (1), (6) and (7), in the CIELAB hue circle.
Legend: ● – Film sample (1) - 1.5% Chitosan (control); ■ Film sample (6) - 1.5% Chitosan + 0.5% Cutin CM_dKA + Tween® 20 (blend); ▲ Film sample (7) - 1.5% Chitosan + 0.5% Cutin CM_dNaA + Tween® 20 (blend).

As expected, the position of the chitosan control film is in the second quadrant of the graph, a quadrant that ranges from yellow to green, while the two cutin and chitosan films are in the first quadrant, which ranges from red to yellow.

To thoroughly evaluate how the incorporation of the depolymerized cutin suspension changed the color of the cutin and chitosan films compared to the chitosan control film, and to what extent this change is detectable to the human eye, the color difference (ΔE^*_{ab}) between the films was calculated (**Table 3.10**).

Table 3.10 - Color difference (ΔE^*_{ab}) values between the chitosan film sample (1) and the two selected cutin and chitosan film samples (6) and (7).

Film samples	Color difference (ΔE^*_{ab})
(1) 1.5% Chitosan (control) & (6) 1.5% Chitosan + 0.5% Cutin CM_dKA + Tween® 20 (blend)	50.07 ± 1.82
(1) 1.5% Chitosan (control) & (7) 1.5% Chitosan + 0.5% Cutin CM_dNaA + Tween® 20 (blend)	42.60 ± 1.93

The ΔE^*_{ab} values obtained were well above one, more precisely 50.07 for film sample (6) and 42.60 for film sample (7). This confirms a significant variation in the colors of the cutin and chitosan films compared to the chitosan film, and that this can be clearly perceived by the human eye.

Water Contact Angle

In order to assess the hydrophobicity of the produced films, the static contact angles between a water droplet and the upper surface of each of the films were measured (**Table 3.11**).

Table 3.11 - Static water contact angle values (θ, °) of the selected film samples.

Film samples	Static water contact angle (θ, °)
(1) 1.5% Chitosan (control)	93.35 ± 0.14
(6) 1.5% Chitosan + 0.5% Cutin CM_dKA + Tween® 20 (blend)	93.37 ± 0.31
(7) 1.5% Chitosan + 0.5% Cutin CM_dNaA + Tween® 20 (blend)	95.15 ± 0.53

The measurements were performed in the upper surface of the films, so the data showed above has no influence of the flat PFA evaporating dish surface where the films were dried. The measurement of the contact angle with a solvent is a way to evaluate the affinity between that solvent and the surface of the material being tested.

Once again, Leceta *et al.* [79] reported a water contact angle result similar to that obtained for the control film of this study. Reaching a value between 90 and 95°, for low molecular weight (LMw) chitosan and 30% $w_{glycerol}/w_{chitosan}$ films.

The results gathered in **Table 3.11** suggest that all the samples revealed similar static water contact angle values for both the control and the cutin and chitosan films. Since high contact angles are characteristic of hydrophobic surfaces, these results suggest that the films produced have a hydrophobic character, even though the incorporation of cutin did not produce a significant increase in the water contact angle of the films, as one might expect.

These values are in line with those of previous studies mentioned in **Section 1.3.3** of this thesis, for other cutin-based films.

Water Vapor Permeability

The water vapor permeability (WVP) results for chitosan (control) and cutin and chitosan blend films for a driving force of 75.5% - 32.8% RH (Relative Humidity) are presented in **Table 3.12**.

Table 3.12 - Water Vapor Permeability values of the selected film samples.

Film samples	WVP $x10^{-11}$ (mol.m/m^2sPa)
(1) 1.5% Chitosan (control)	5.33 ± 1.66
(6) 1.5% Chitosan + 0.5% Cutin CM_dKA + Tween® 20 (blend)	3.84 ± 0.39
(7) 1.5% Chitosan + 0.5% Cutin CM_dNaA + Tween® 20 (blend)	6.20 ± 2.44

The WVP parameter is a very important parameter, especially if these films are to be used for food packaging. However, it is also a very challenging parameter to compare, since the WVP is highly dependent on a number of factors, including film thickness, the driving force used in the assay, the concentration and type of plasticizer used, other additives added, molecular weight of the polymer, etc. [84]

The chitosan film (control) presented a WVP value of (5.33 ± 1.66) $x10^{-11}$ (mol.m/m^2sPa), which was higher than the (4.13 ± 0.13) $x10^{-11}$ (mol.m/m^2sPa) value reported by Ferreira *et al.* (2016) for a film with 1.5% (w/w) chitosan, 30% $w_{glycerol}/w_{chitosan}$ and 50% $w_{citric\ acid}/w_{chitosan}$ and a driving force of 76.9–22.5% RH.

The cutin and chitosan film sample (6) obtained the lowest value of WVP, of (3.84 ± 0.39) $x10^{-11}$ (mol.m/m^2sPa), while the film sample (7) presented a value slightly higher than that of the control.

Tedeschi *et al.* [16] reported an improvement in barrier properties, including WVP, of films composed of sodium alginate, fatty acids of tomato pomace and beeswax. The authors observed a decrease in the WVP parameter with the proportion of tomato pomace monomers, attributing this result to the hydrophobic nature of the polyhydroxylated and unsaturated long-chain fatty acids of tomato pomace.

While the result obtained for film sample (6) matches those observed by Tedeschi *et al.* (2018), film sample (7) doesn't, which may be related to the lower uniformity and homogeneity of this film when compared to film (6) observed earlier (**Figure 3.2**).

4. Conclusions

The massive increase in food processing waste and the urgent need to replace conventional plastics in packaging applications are major problems of the present time. The work developed in this thesis aims to develop an alternative involving biodegradable materials, based on cutin and to replace conventional plastics for packaging.

Tomato pomace, a waste product from the tomato processing industry, was characterized regarding its moisture content (84.07 ± 0.42% w/w) and its fractional composition (63.62 ± 1.85% peel, 34.59 ± 2.51% seed, and 1.80 ± 0.73% fiber, w/w).

Several methods for extracting and depolymerizing cutin, a biopolymer of the tomato cuticle, were explored. Methods differed in the state of the initial raw material (humid tomato peels *versus* dried and milled tomato peels), the existence of a tomato peel dewaxing step and the type of solvent used for this purpose (acetone:ethanol mixture *versus* heptane), alkaline hydrolysis solution (aqueous NaOH solution *versus* ethanolic KOH solution) and isolation strategy of the cutin monomers (acidification *versus* nanofiltration).

Monomeric extracts of cutin were successfully obtained and confirmed to be enriched in several fatty acids, including 16-hydroxy-hexadecanoic acid, hexadecanedioic acid, stearic acid, linoleic acid, palmitic acid, octadecanedioic acid and oleic acid. Extracts CM_dNaA and CM_dKA, the former obtained by hydrolysis of dried and milled tomato peels with an aqueous NaOH solution followed by monomer recovery by acidification and the latter obtained by hydrolysis of dried, milled and dewaxed tomato peels with an ethanolic solution of KOH followed by monomer recovery by acidification, had the highest mass percentage of total fatty acid per mass of freeze-dried extract, respectively, 24.71% and 8.22%.

Cutin and chitosan-based films were prepared from these two extracts of recovered tomato cutin monomers (CM_dKA and CM_dNaA) and commercial chitosan by casting and drying at 40°C. Two strategies of film production were performed, resulting in two types of films — blend of cutin and chitosan and bilayer films. Cutin and chitosan blend films were the most malleable and homogeneous.

Cutin and chitosan blend films were characterized regarding its thickness (0.103 ± 0.004mm and 0.106 ± 0.005mm), color, water contact angle (93.37 ± 0.31° and 95.15 ± 0.53°) and water vapor permeability ((3.84 ± 0.39) $x10^{-11}$ mol.m/m^2sPa and (6.20 ± 2.44) $x10^{-11}$ mol.m/m^2sPa).

The hydrophobic films produced in the course of this study undoubtedly show great potential, even though some improvements are needed before starting to replace food packaging made from petroleum-based polymers. In addition, they may provide an application for tomato processing waste, making the process of tomato production and processing more profitable and sustainable.

5. Future Work

Given that the cutin and chitosan-based films produced in this work have shown such promising characteristics, it is of great interest to not only optimize the work done so far by deepening certain issues, such as further characterizing the monomeric cutin extracts, but also to investigate beyond what has been achieved.

In light of this, it is suggested:

- Further characterization of the monomeric cutin extracts, not only for their remaining fatty acid profile, but also for the presence of waxes, polysaccharides, and phenolic compounds;
- Further optimization of the bilayer film-forming strategy. Obtaining homogeneous bilayer films of cutin and chitosan would be very interesting, in the sense that one surface of the film would possess the properties of chitosan (e.g. antimicrobial and antioxidant activities) and the other surface the properties of cutin (e.g. hydrophobicity and UV-blocking capacities);
- Characterization of the films regarding UV-Vis radiation barrier capacity, moisture content, solubility (especially water), antioxidant activity, mechanical properties (tensile and perforation tests) and gas permeability (especially O_2);
- Application of the films in fresh fruits and vegetables by wrapping them with it, in order to study the film's performance in preserving the food and extending shelf life.

6. References

[1] Y. F. Tsang *et al.*, “Production of bioplastic through food waste valorization,” *Environ. Int.*, vol. 127, pp. 625–644, Jun. 2019.

[2] J. H. Clark, R. Luque, and A. S. Matharu, “Green chemistry, biofuels, and biorefinery,” *Annu. Rev. Chem. Biomol. Eng.*, vol. 3, pp. 183–207, Jul. 2012.

[3] M. Sharma, Z. Usmani, V. K. Gupta, and R. Bhat, “Valorization of fruits and vegetable wastes and by-products to produce natural pigments,” *https://doi.org/10.1080/07388551.2021.1873240*, vol. 41, no. 4, pp. 535–563, 2021.

[4] L. Bhatia, S. Johri, and R. Ahmad, “An economic and ecological perspective of ethanol production from renewable agro waste: a review,” *AMB Express*, vol. 2, no. 1, pp. 1–19, 2012.

[5] V. K. Joshi, A. Kumar, and V. Kumar, “Antimicrobial, antioxidant and phyto-chemicals from fruit and vegetable wastes: A review,” *Intl. J. Food. Ferment. Technol*, vol. 2, no. 2, pp. 123–136, 2012.

[6] E. El-Tanboly and M. El-Hofi, “Recovery of cheese whey, a by-product from the dairy industry for use as an animal feed,” *J. Nutr. Heal. Food Eng.*, vol. 6, no. 5, pp. 148–154, Jun. 2017.

[7] I. K. Lappa *et al.*, “Cheese Whey Processing: Integrated Biorefinery Concepts and Emerging Food Applications,” *Foods*, vol. 8, no. 8, pp. 1–37, Aug. 2019.

[8] J. J. Benítez *et al.*, “Valorization of Tomato Processing by-Products: Fatty Acid Extraction and Production of Bio-Based Materials,” *Mater. (Basel, Switzerland)*, vol. 11, no. 11, pp. 1–13, Nov. 2018.

[9] M. R. Ventura, M. C. Pieltain, and J. I. R. Castanon, “Evaluation of tomato crop by-products as feed for goats,” *Anim. Feed Sci. Technol.*, vol. 154, no. 3, pp. 271–275, 2009.

[10] C. Yuangklang *et al.*, “Growth performance in beef cattle fed rations containing dried tomato pomace,” *J. Anim. Vet. Adv.*, vol. 9, no. 17, pp. 2261–2264, 2010.

[11] Z. Lu, J. Wang, R. Gao, F. Ye, and G. Zhao, “Sustainable valorisation of tomato pomace: A comprehensive review,” *Trends in Food Science and Technology*, vol. 86. pp. 172–187, 2019.

[12] V. Lavelli and M. C. Torresani, “Modelling the stability of lycopene-rich by-products of tomato processing,” *Food Chem.*, vol. 125, no. 2, pp. 529–535, 2011.

[13] A. Costa *et al.*, “Evaluating the presence of lycopene-enriched extracts from tomato on topical emulsions: Physico-chemical characterization and sensory analysis,” *Appl. Sci.*, vol. 11, no. 11, pp. 1–18, 2021.

[14] M. Y. Ali *et al.*, “Nutritional composition and bioactive compounds in tomatoes and their impact on human health and disease: A review,” *Foods*, vol. 10, no. 1, pp. 1–32, 2021.

[15] J. A. Heredia-Guerrero *et al.*, “Cutin from agro-waste as a raw material for the production of bioplastics,” *J. Exp. Bot.*, vol. 68, no. 19, pp. 5401–5410, Nov. 2017.

[16] G. Tedeschi *et al.*, “Sustainable Fabrication of Plant Cuticle-Like Packaging Films from Tomato Pomace Agro-Waste, Beeswax, and Alginate,” *ACS Sustain. Chem. Eng.*, vol. 6, no. 11, pp. 14955–14966, Nov. 2018.

[17] FAO, “FAOSTAT Online (FAO Statistical Databases),” *Food & Agriculture Organization of the United Nations (FAO)*, 2022. [Online]. Available: http://apps.fao.org/. [Accessed: 11-Jan-2022].

[18] I. Kakabouki *et al.*, “Evaluation of Processing Tomato Pomace after Composting on Soil Properties, Yield, and Quality of Processing Tomato in Greece,” *Agronomy*, vol. 11, no. 1, p. 88, Jan. 2021.

[19] S. Trombino, R. Cassano, D. Procopio, M. L. Di Gioia, and E. Barone, “Valorization of tomato waste as a source of carotenoids,” *Molecules*, vol. 26, no. 16. p. 5062, 2021.

[20] C. Rock, W. Yang, R. Goodrich-Schneider, and H. Feng, “Conventional and Alternative Methods for Tomato Peeling,” *Food Eng. Rev.*, vol. 4, no. 1, pp. 1–15, Mar. 2012.

[21] J. M. Costa and E. Heuvelink, *Tomatoes*, 2nd ed. CABI, 2018.

[22] M. J. Díez and F. Nuez, “Tomato,” in *Vegetables II*, 1st ed., Jaime Prohens-Tomás and Fernando Nuez, Eds. New York, NY: Springer New York, 2008, pp. 249–323.

[23] “Tomatoes,” *Produce Market Guide*. [Online]. Available: https://www.producemarketguide.com/produce/tomatoes. [Accessed: 11-Jan-2022].

[24] Z. Pan, R. Zhang, and S. Zicari, *Integrated Processing Technologies for Food and Agricultural By-Products*, 1st ed. 2019.

[25] WPTC (World Processing Tomato Council), “WPTC Crop update as of 21 October 2021,” *WPTC*, 21-Oct-2021. [Online]. Available: https://www.wptc.to/pdf/releases/WPTC crop update as of 21 october 2021.pdf. [Accessed: 12-Jan-2022].

[26] JBT, “Tomato & Fruit Processing System,” *JBT*, 2022. [Online]. Available: https://www.jbtc.com/foodtech/wp-content/uploads/sites/2/2021/08/Tomato-Fruit-PS_601-EN.pdf. [Accessed: 15-Jan-2022].

[27] Z. Pan *et al.*, “A pilot scale electrical infrared dry-peeling system for tomatoes: Design and performance evaluation,” *Biosyst. Eng.*, vol. 137, pp. 1–8, 2015.

[28] V. Kumar *et al.*, “Peeling of tough skinned fruits and vegetables: A review,” *Int. J. Chem. Stud.*, vol. 7, no. 2, pp. 1825–1829, 2019.

[29] M. Del Valle, M. Cámara, and M. E. Torija, “Chemical characterization of tomato pomace,” *J. Sci. Food Agric.*, vol. 86, no. 8, pp. 1232–1236, 2006.

[30] N. Kalogeropoulos, A. Chiou, V. Pyriochou, A. Peristeraki, and V. T. Karathanos, “Bioactive phytochemicals in industrial tomatoes and their processing byproducts,” *LWT - Food Sci. Technol.*, vol. 49, no. 2, pp. 268–277, 2012.

[31] M. Ahmad Bhat and H. Ahsan, “Quality Characteristics of Freeze and Cabinet Dried Tomato Pomace,” *Int. J. Pure App. Biosci*, vol. 6, no. 2, pp. 891–897, 2018.

[32] Y. P. A. Silva *et al.*, “Characterization of tomato processing by-product for use as a potential functional food ingredient: nutritional composition, antioxidant activity and bioactive compounds,” *Int. J. Food Sci. Nutr.*, vol. 70, no. 2, pp. 150–160, 2019.

[33] D. Kaur, D. S. Sogi, S. K. Garg, and A. S. Bawa, “Flotation-cum-sedimentation system for skin and seed separation from tomato pomace,” *J. Food Eng.*, vol. 71, no. 4, pp. 341–344, 2005.

[34] V. Nour, T. D. Panaite, M. Ropota, R. Turcu, I. Trandafir, and A. R. Corbu, “Nutritional and bioactive compounds in dried tomato processing waste,” *CYTA - J. Food*, vol. 16, no. 1, pp. 222–229, 2018.

[35] K. Gebeyew, G. Animut, M. Urge, and T. Feyera, “The Effect of Feeding Dried Tomato Pomace and Concentrate Feed on Body Weight Change, Carcass Parameter and Economic Feasibility on Hararghe Highland Sheep, Eastern Ethiopia,” *J Vet. Sci Technolo*, vol. 6, no. 2, p. 1000217, 2015.

[36] I. Gheonea *et al.*, “Investigations on thermostability of carotenoids from tomato peels in oils using a kinetic approach,” *J. Food Process. Preserv.*, vol. 44, no. 1, p. e14303, Jan. 2020.

[37] N. Baaka, I. El Ksibi, and M. F. Mhenni, “Optimisation of the recovery of carotenoids from tomato processing wastes: application on textile dyeing and assessment of its antioxidant activity,” *Nat. Prod. Res.*, vol. 31, no. 2, pp. 196–203, 2017.

[38] A. M. Giuffrè *et al.*, “Tomato seed oil for biodiesel production,” *Eur. J. Lipid Sci. Technol.*, vol. 118, no. 4, pp. 640–650, Apr. 2016.

[39] Y. Li, Y. Li, D. Zhang, G. Li, J. Lu, and S. Li, “Solid state anaerobic co-digestion of tomato residues with dairy manure and corn stover for biogas production,” *Bioresour. Technol.*, vol. 217, pp. 50–55, Oct. 2016.

[40] M. do Rosário Freixo, A. Karmali, and J. M. Arteiro, “Production, purification and characterization of laccase from Pleurotus ostreatus grown on tomato pomace,” *World J. Microbiol. Biotechnol.*, vol. 28, no. 1, pp. 245–254, 2012.

[41] M. A. Umsza-Guez, A. B. Díaz, I. de Ory, A. Blandino, E. Gomes, and I. Caro, “Xylanase production by Aspergillus awamori under solid state fermentation conditions on tomato pomace,” *Brazilian J. Microbiol.*, vol. 42, no. 4, pp. 1585–1597, 2011.

[42] M. S. Y. Haddadin, I. M. Abu-Reesh, F. A. S. Haddadin, and R. K. Robinson, “Utilisation of tomato pomace as a substrate for the production of vitamin B12 - A preliminary appraisal,” *Bioresour. Technol.*, vol. 78, no. 3, pp. 225–230, 2001.

[43] O. Güneşer, A. Demirkol, Y. Karagül Yüceer, S. Özmen Toğay, M. İşleten Hoşoğlu, and M. Elibol, “Bioflavour production from tomato and pepper pomaces by Kluyveromyces marxianus and Debaryomyces hansenii,” *Bioprocess Biosyst. Eng.*, vol. 38, no. 6, pp. 1143–1155, 2015.

[44] I. Kakabouki, A. Efthimiadou, A. Folina, C. Zisi, and S. Karydogianni, “Effect of different tomato pomace compost as organic fertilizer in sweet maize crop,” *https://doi.org/10.1080/00103624.2020.1853148*, vol. 51, no. 22, pp. 2858–2872, 2020.

[45] A. Manfredini, A. Chiariotti, E. Santangelo, E. Rossi, G. Renzi, and M. T. Dell’Abate, “Assessing the Biological Value of Soluble Organic Fractions from Tomato Pomace Digestates,” *J. Soil Sci. Plant Nutr.*, vol. 21, no. 1, pp. 301–314, Mar. 2021.

[46] L. B. B. Martin and J. K. C. Rose, “There’s more than one way to skin a fruit: formation and functions of fruit cuticles,” *J. Exp. Bot.*, vol. 65, no. 16, pp. 4639–4651, Aug. 2014.

[47] E. Dominguez, J. A. Heredia-Guerrero, and A. Heredia, “The biophysical design of plant cuticles: an overview,” *New Phytol.*, vol. 189, no. 4, pp. 938–949, Mar. 2011.

[48] A. Cifarelli, I. M. Cigognini, L. Bolzoni, and A. Montanari, “Physical-Chemical Characteristics of Cutin Separated from Tomato Waste for the Preparation of Bio-lacquers,” *Adv. Sci. Eng.*, vol. 11, no. 1, pp. 33–45, Jun. 2019.

[49] M. B. Gómez-Patiño, R. Estrada-Reyes, M. E. Vargas-Diaz, and D. Arrieta-Baez, “Cutin from Solanum Myriacanthum Dunal and Solanum Aculeatissimum Jacq. as a Potential Raw Material for Biopolymers,” *Polymers (Basel).*, vol. 12, no. 9, p. 1945, Aug. 2020.

[50] J. A. Heredia-Guerrero *et al.*, “Infrared spectroscopy as a tool to study plant cuticles,” vol. 28, no. 2, pp. 10–13, 2016.

[51] E. A. Fich, N. A. Segerson, and J. K. C. Rose, “The Plant Polyester Cutin: Biosynthesis, Structure, and Biological Roles,” *Annu. Rev. Plant Biol.*, vol. 67, pp. 207–233, Apr. 2016.

[52] S. Hauff, B. Chefetz, M. Shechter, and W. Vetter, “Determination of hydroxylated fatty acids from the biopolymer of tomato cutin and their fate during incubation in soil,” *Phytochem. Anal.*, vol. 21, no. 6, pp. 582–589, Nov. 2010.

[53] C. J. S. Moreira *et al.*, “An Ionic Liquid Extraction That Preserves the Molecular Structure of Cutin Shown by Nuclear Magnetic Resonance,” *Plant Physiol.*, vol. 184, no. 2, pp. 592–606, Oct. 2020.

[54] S. Guzmán-Puyol, A. Heredia, J. A. Heredia-Guerrero, and J. J. Benítez, “Cutin-Inspired Polymers and Plant Cuticle-like Composites as Sustainable Food Packaging Materials,” *Sustain. Food Packag. Technol.*, pp. 161–198, Mar. 2021.

[55] PubChem, “10,16-Dihydroxyhexadecanoic acid | C16H32O4 - PubChem,” 2022. [Online]. Available: https://pubchem.ncbi.nlm.nih.gov/compound/441449. [Accessed: 12-Feb-

2022].

[56] PubChem, “7-Hydroxyhexadecanedioic acid | C16H30O5 - PubChem,” 2022. [Online]. Available: https://pubchem.ncbi.nlm.nih.gov/compound/14259008. [Accessed: 12-Feb-2022].

[57] PubChem, “8-Hydroxyhexadecanedioic acid | C16H30O5 - PubChem,” 2022. [Online]. Available: https://pubchem.ncbi.nlm.nih.gov/compound/16061042. [Accessed: 12-Feb-2022].

[58] PubChem, “16-Hydroxyhexadecanoic acid | C16H32O3 - PubChem,” 2022. [Online]. Available: https://pubchem.ncbi.nlm.nih.gov/compound/10466. [Accessed: 12-Feb-2022].

[59] PubChem, “Palmitic acid | C16H32O2 - PubChem,” 2022. [Online]. Available: https://pubchem.ncbi.nlm.nih.gov/compound/985. [Accessed: 12-Feb-2022].

[60] PubChem, “Linoleic acid | C18H32O2 - PubChem,” 2022. [Online]. Available: https://pubchem.ncbi.nlm.nih.gov/compound/5280450. [Accessed: 12-Feb-2022].

[61] PubChem, “Oleic acid | C18H34O2 - PubChem,” 2022. [Online]. Available: https://pubchem.ncbi.nlm.nih.gov/compound/445639. [Accessed: 12-Feb-2022].

[62] H. de Vries, G. Bredemeijer, and W. Heinen, “The decay of cutin and cuticular components by soil microorganisms in their natural environment,” *Acta Bot. Neerl.*, vol. 16, no. 3, pp. 102–110, 1967.

[63] I. Cigognini, A. Montanari, and R. De La Torre Carreras, “Extraction method of a polyester polymer or cutin from the wasted tomato peels and polyester polimer so extracted.,” WO 2015/028299 Al, 05-Mar-2015.

[64] M. Marc *et al.*, “Bioinspired co-polyesters of hydroxy-fatty acids extracted from tomato peel agro-wastes and glycerol with tunable mechanical, thermal and barrier properties,” *Ind. Crops Prod.*, vol. 170, p. 113718, Oct. 2021.

[65] A. Manrich, F. K. V. Moreira, C. G. Otoni, M. V. Lorevice, M. A. Martins, and L. H. C. Mattoso, “Hydrophobic edible films made up of tomato cutin and pectin,” *Carbohydr. Polym.*, vol. 164, pp. 83–91, May 2017.

[66] P. Wang, P. Fei, C. Zhou, and P. Hong, “Stearic acid esterified pectin: Preparation, characterization, and application in edible hydrophobic pectin/chitosan composite films,” *Int. J. Biol. Macromol.*, vol. 186, pp. 528–534, Sep. 2021.

[67] Y. Ye, F. Zeng, M. Zhang, S. Zheng, J. Li, and P. Fei, “Hydrophobic edible composite packaging membrane based on low-methoxyl pectin/chitosan: Effects of lotus leaf cutin,” *Food Packag. Shelf Life*, vol. 26, p. 100592, Dec. 2020.

[68] C. Hood, T. Laredo, A. G. Marangoni, and E. Pensini, “Water-repellent films from corn protein and tomato cutin,” *J. Appl. Polym. Sci.*, vol. 138, no. 33, p. 50831, Sep. 2021.

[69] V. Varžinskas and Z. Markevičiūtė, “Sustainable Food Packaging: Materials and Waste Management Solutions,” *Environ. Res. Eng. Manag.* , vol. 76, no. 3, pp. 154–164, Sep. 2020.

[70] P. R. Salgado, L. Di Giorgio, Y. S. Musso, and A. N. Mauri, “Recent Developments in Smart Food Packaging Focused on Biobased and Biodegradable Polymers,” *Front. Sustain. Food Syst.*, vol. 5, p. 125, Apr. 2021.

[71] K. Marsh and B. Bugusu, “Food Packaging—Roles, Materials, and Environmental Issues,” *J. Food Sci.*, vol. 72, no. 3, pp. R39–R55, Apr. 2007.

[72] Eurostat - Statistics Explained, “Packaging waste statistics,” *Eurostat - Statistics Explained*, 2022. [Online]. Available: https://ec.europa.eu/eurostat/statistics-explained/index.php?title=Packaging_waste_statistics#Conclusions. [Accessed: 05-Feb-2022].

[73] A. R. V. Ferreira, V. D. Alves, and I. M. Coelhoso, “Polysaccharide-Based Membranes in

Food Packaging Applications," *Membranes (Basel).*, vol. 6, no. 2, pp. 1–17, Apr. 2016.

[74] European Bioplastics, "Bioplastic materials," *European Bioplastics*, 2022. [Online]. Available: https://www.european-bioplastics.org/bioplastics/materials/. [Accessed: 05-Feb-2022].

[75] T. Iwata, "Biodegradable and Bio-Based Polymers: Future Prospects of Eco-Friendly Plastics," *Angew. Chemie Int. Ed.*, vol. 54, no. 11, pp. 3210–3215, Mar. 2015.

[76] L. Shen, E. Worrell, and M. Patel, "Present and future development in plastics from biomass," *Biofuels, Bioprod. Biorefining*, vol. 4, no. 1, pp. 25–40, Jan. 2010.

[77] H. Wang, J. Qian, and F. Ding, "Emerging Chitosan-Based Films for Food Packaging Applications," *J. Agric. Food Chem.*, vol. 66, no. 2, pp. 395–413, Jan. 2018.

[78] M. Z. Elsabee and E. S. Abdou, "Chitosan based edible films and coatings: A review," *Mater. Sci. Eng. C*, vol. 33, no. 4, pp. 1819–1841, May 2013.

[79] I. Leceta, P. Guerrero, and K. De La Caba, "Functional properties of chitosan-based films," *Carbohydr. Polym.*, vol. 93, no. 1, pp. 339–346, Mar. 2013.

[80] I. Leceta, P. Guerrero, I. Ibarburu, M. T. Dueñas, and K. De La Caba, "Characterization and antimicrobial analysis of chitosan-based films," *J. Food Eng.*, vol. 116, no. 4, pp. 889–899, Jun. 2013.

[81] S. Beigzadeh Ghelejlu, M. Esmaiili, and H. Almasi, "Characterization of chitosan-nanoclay bionanocomposite active films containing milk thistle extract," *Int. J. Biol. Macromol.*, vol. 86, pp. 613–621, May 2016.

[82] Y. Peng and Y. Li, "Combined effects of two kinds of essential oils on physical, mechanical and structural properties of chitosan films," *Food Hydrocoll.*, vol. 36, pp. 287–293, May 2014.

[83] A. B. Lanham *et al.*, "Determination of the extraction kinetics for the quantification of polyhydroxyalkanoate monomers in mixed microbial systems," *Process Biochem.*, vol. 48, no. 11, pp. 1626–1634, Nov. 2013.

[84] A. R. V. Ferreira *et al.*, "Development and characterization of bilayer films of FucoPol and chitosan," *Carbohydr. Polym.*, vol. 147, pp. 8–15, Aug. 2016.

[85] B. C. K. Ly, E. B. Dyer, J. L. Feig, A. L. Chien, and S. Del Bino, "Research Techniques Made Simple: Cutaneous Colorimetry: A Reliable Technique for Objective Skin Color Measurement," *J. Invest. Dermatol.*, vol. 140, no. 1, pp. 3-12.e1, Jan. 2020.

7. Appendix

7.1 Characterization of the Monomeric Cutin Extracts (GC-FID)

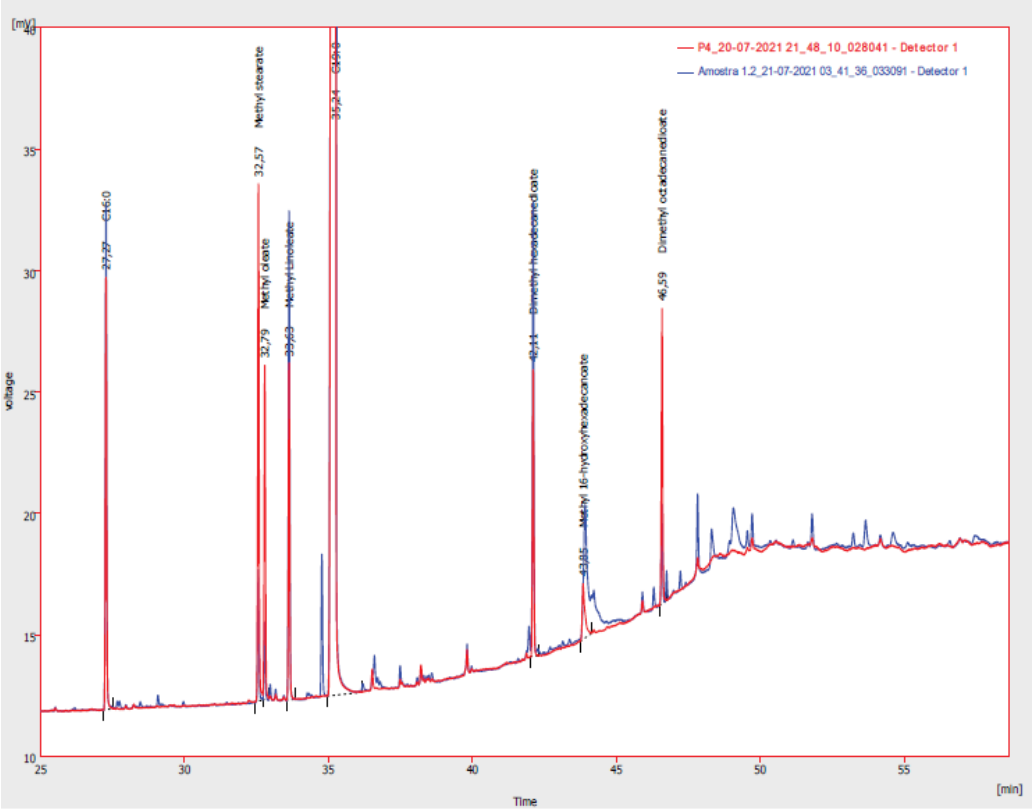

Figure A.1 - Chromatogram of the monomeric cutin extract CM_wNaA (Group 1).

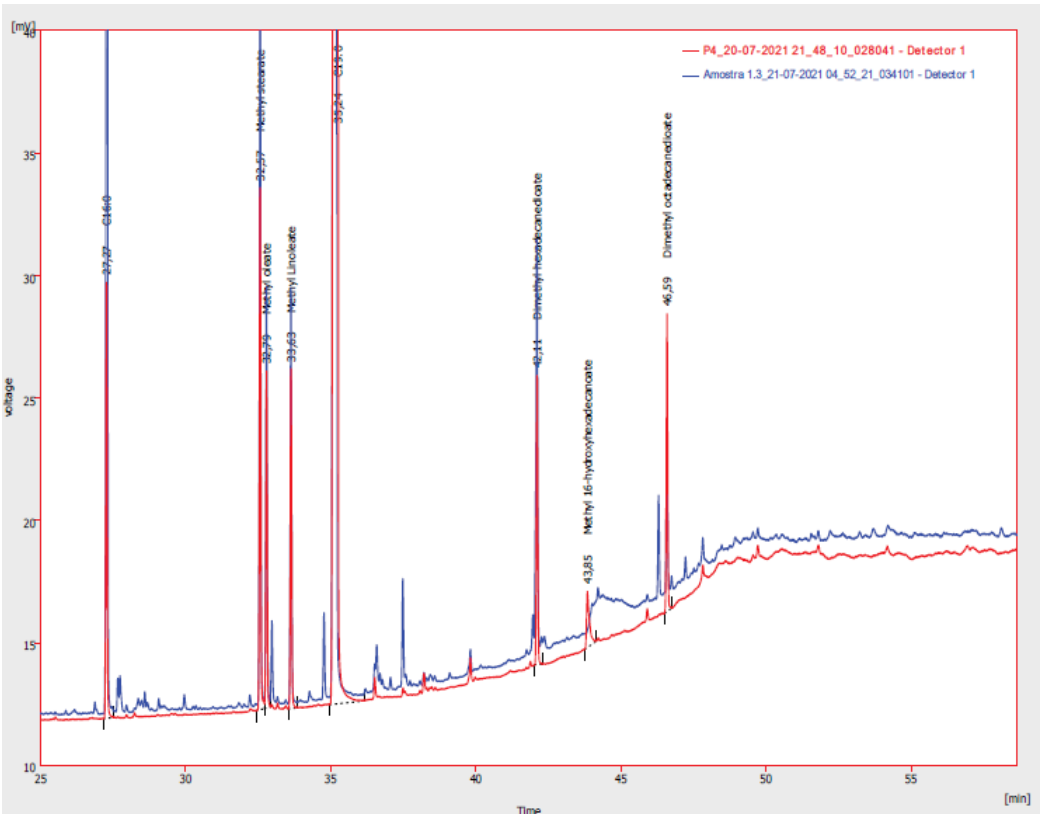

Figure A.2 - Chromatogram of the monomeric cutin extract CM_dNaA (Group 1).

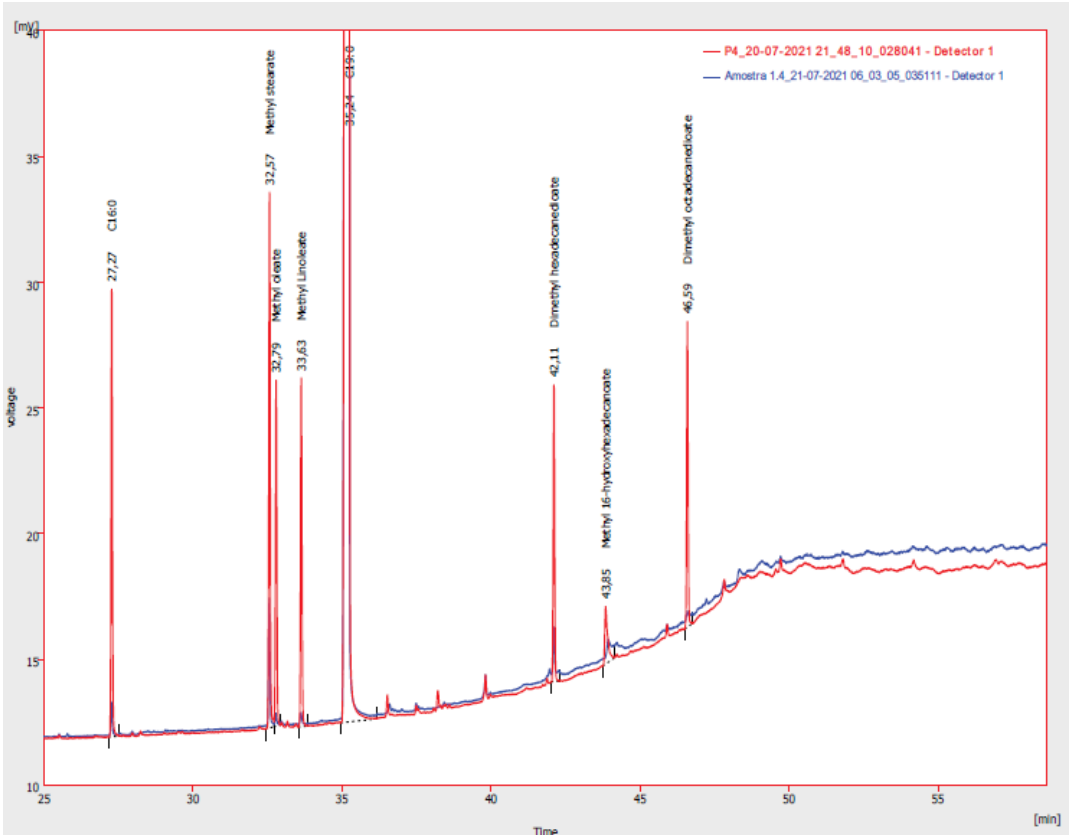

Figure A.3 - Chromatogram of the monomeric cutin extract CM_wNaNP010 (Group 1).

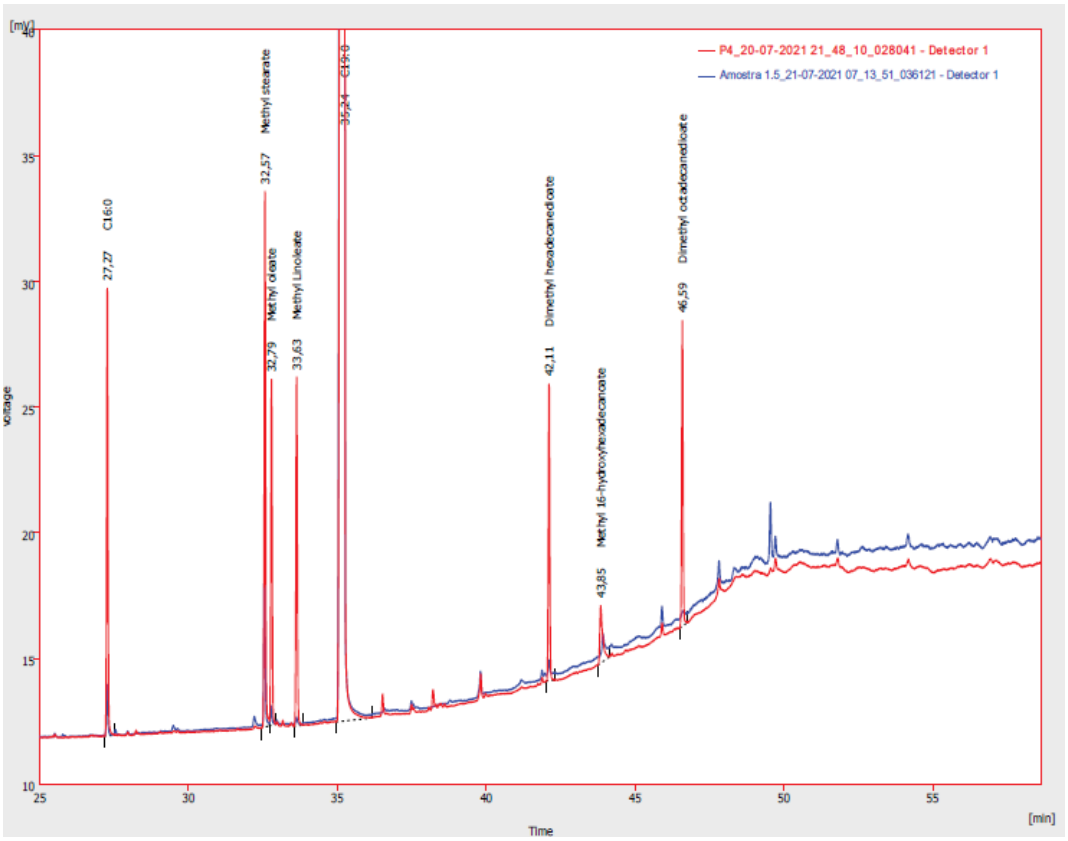

Figure A.4 - Chromatogram of the monomeric cutin extract CM_wNaNP030 (Group 1).

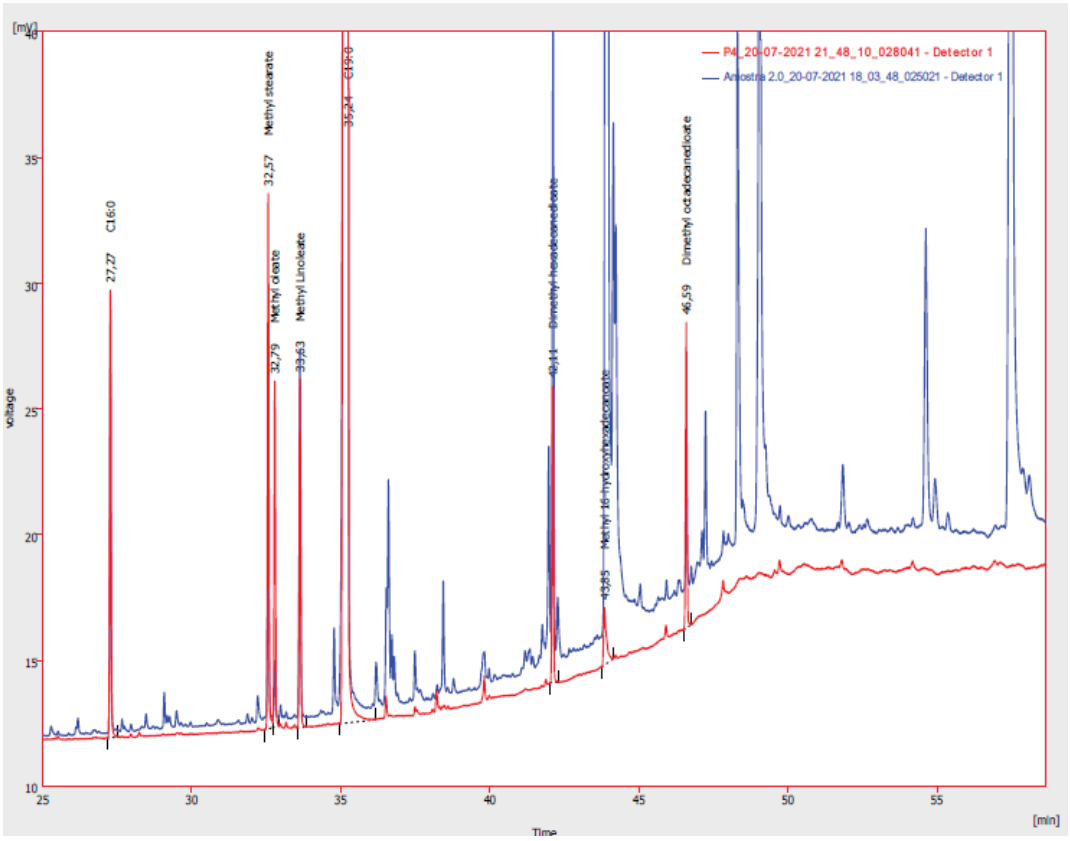

Figure A.5 - Chromatogram of the monomeric cutin extract CM_dKA (Group 2).

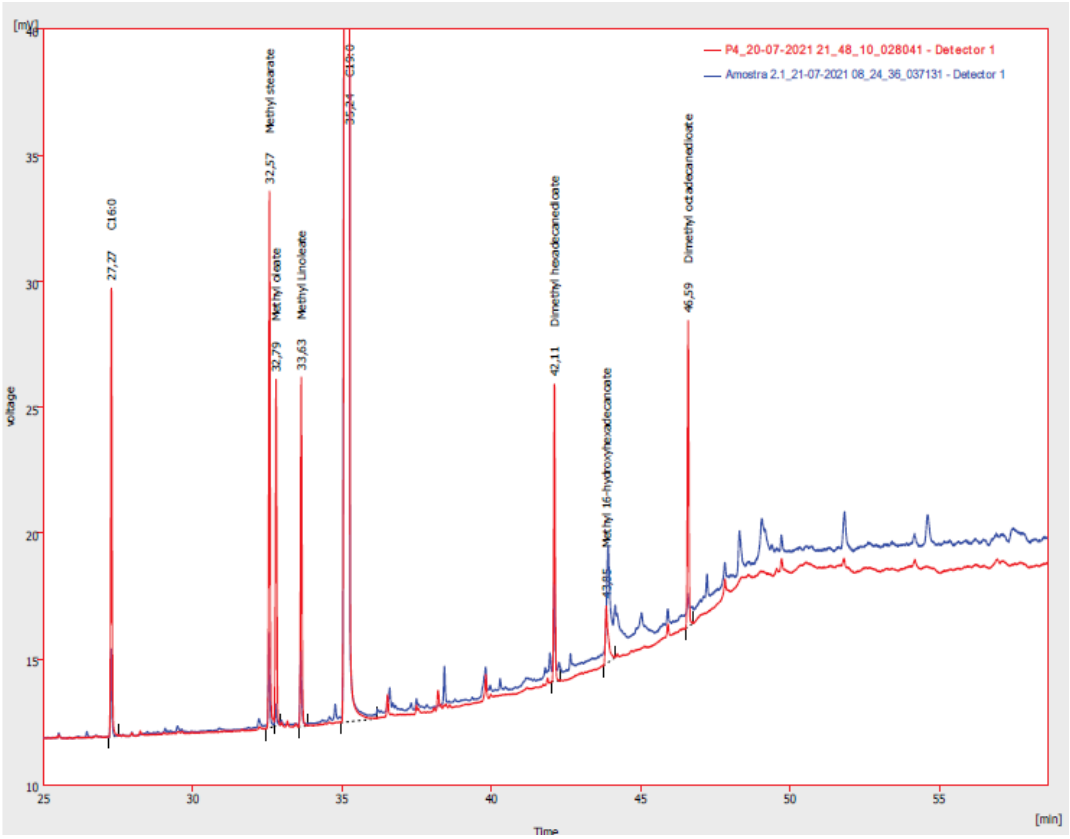

Figure A.6 - Chromatogram of the monomeric cutin extract CM_dKNP010 (Group 2).

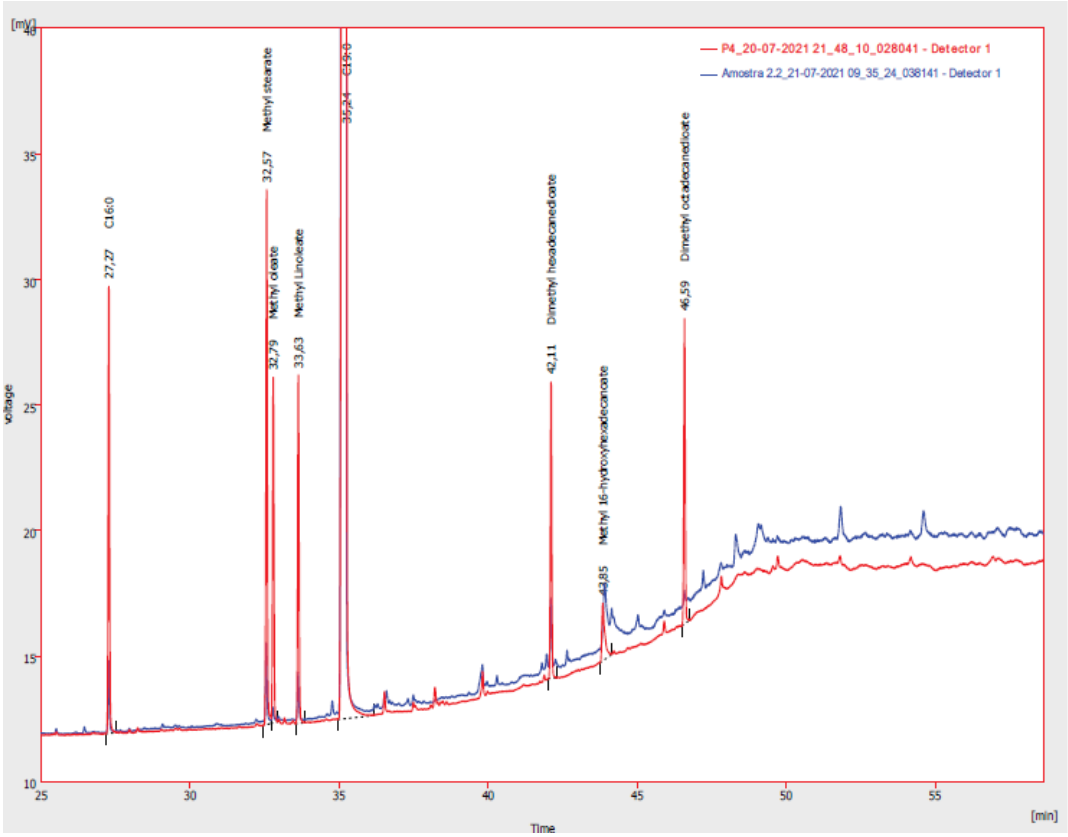

Figure A.7 - Chromatogram of the monomeric cutin extract CM_dKNP030 (Group 2).

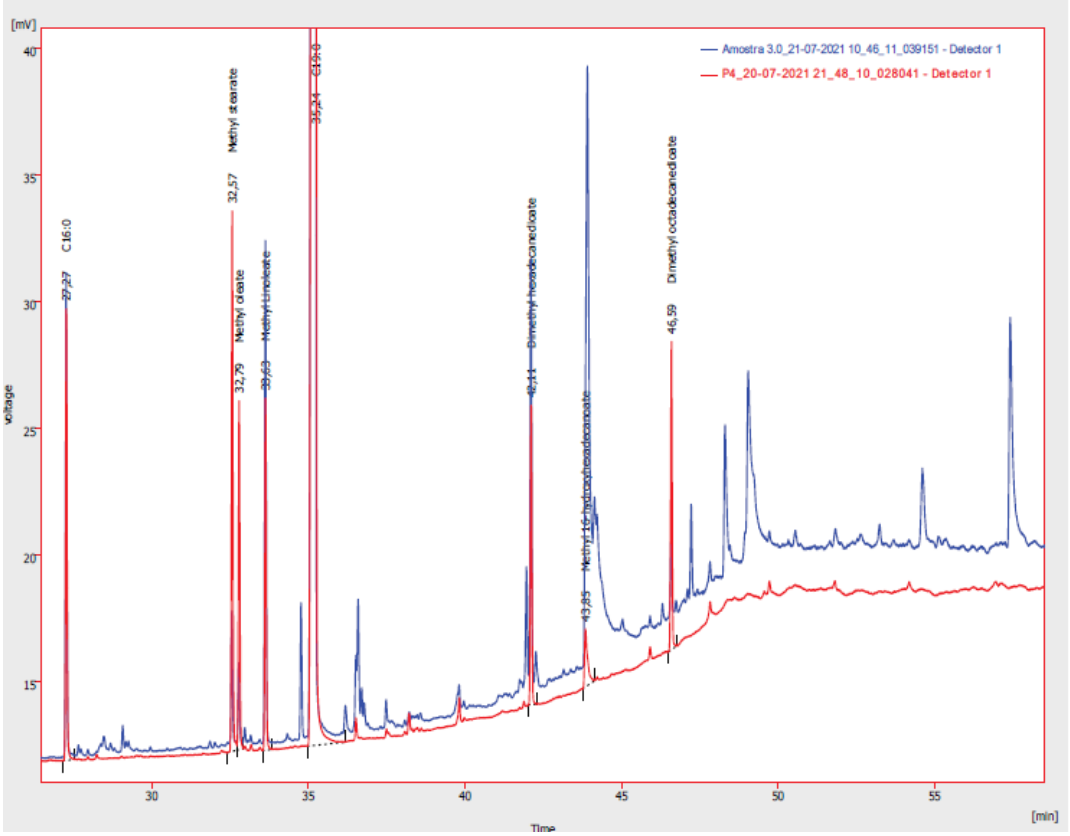

Figure A.8 - Chromatogram of the monomeric cutin extract CM_dheptKA (Group 3).

2022

ANDREIA FILIPA MORAIS SIMÕES

RECOVERY AND PURIFICATION OF CUTIN FROM TOMATO BY-PRODUCTS FOR APPLICATION IN HYDROPHOBIC FILMS

NOVA SCHOOL OF SCIENCE & TECHNOLOGY